ALUMINOSILICATE-COATED SILICA SAND FOR REACTIVE TRANSPORT EXPERIMENTS

By

JORGE ANTONIO JEREZ BRIONES

A dissertation submitted in partial fulfillment of
the requirements for the degree of

DOCTOR OF PHILOSOPHY

WASHINGTON STATE UNIVERSITY
Program of Engineering Science

May 2005

To the Faculty of Washington State University:

The members of the Committee appointed to examine the dissertation of Jorge Jerez find it satisfactory and recommend that it be accepted.

_____

Co-Chair

_____

Co-Chair

_____

Acknowledgement

I express my sincere appreciation to those who have assisted me during the course of this study. Especially I would like to thank the members of my dissertation committee Dr. Claudio Stockle, Dr. Markus Flury and Dr. Brent Peyton for their consistent support, ideas, and discussions during these years. Especially I thanks to Dr. Markus Flury who was my direct supervisor and who provide valuable discussions during all the experimental research. The time and effort that he invests in my scientific formation, as well his friendship has produced in me a deep appreciation for him.

I am also indebted to Dr. Youjun Deng with whom I discussed and from whom I received very thoughtful comments about polymer-clay interactions; to Jianying Shang who made contact angle measurements and help me collecting data for humic acid transport experiments; Dr. Barbara Williams and Jason Shira from University of Idaho for providing access and technical advise in the use of the Field Flow Fractionation instrument. I am also grateful to Chris Davitt and Valerie Lynch-Holm from the Electron Microscopy Center at Washington State University for their assistance during the used of the scanning electron microscope. I also thank the people of the Department of Crop and Soil Science, who hosted me during all my experimental research, especially to Jon Mathison, Jeffrey Boyle, and Mary Fauci; Naomi Calkins-Golter from the Department of Chemical Engineering provided technical support and constructive

suggestions during my experiments, and Dr. Gang Chen who conducted all the surface area analyses.

The opportunity to pursue my graduate studies was provided by the Government of Chile through the Agriculture Research Institute (INIA), through its financial support.

During my studies I received the support of my friends and graduate student fellows. Thanks are given to Szabolcs Czigány, Jarai Mon, Celso Oie, Victor Alba, and Gabriel Mancilla for their invaluable and warm friendship. Many people from the Pullman community have support me and my family during these years and have made this an unforgettable time in our lives, many thanks to Dean and Mary Guenther and Dustin and Mary Baker.

This work will be not accomplished without the love, help and support of my wife Susana and our children Sara and Vicente. To them and to my parents many thanks.

ALUMINOSILICATE-COATED SILICA SAND FOR REACTIVE TRANSPORT EXPERIMENTS

Abstract

by Jorge Antonio Jerez Briones, Ph.D.
Washington State University
May 2005

Co-Chair: Claudio Stockle

Co-Chair: Markus Flury

Column experiments with pure minerals as porous medium are valuable tools to deduce mechanistic information on the fate and transport of reactive chemicals in the subsurface. Most commonly, silica sand is used as the model porous medium. Iron oxides have been used as well, mainly in form of iron-oxide-coated silica sand. Clay minerals, however, have only been recently used as model porous media, and the coating of aluminosilicate clay minerals on silica still needs investigation.

The objectives of this dissertation were (1) to develop a methodology to immobilize aluminosilicate clays (Georgia Kaolinite, Texas Smectite, and Morris Illite) on silica sand, (2) to study the hydrodynamic properties of the modified silica sand when packed into columns, and (3) to examine the fate and transport of humic acid in porous media dominated by different types of clay minerals.

We developed a method to immobilize the clay minerals on a silica support. Two

polymers were used as bridging agents between the clay minerals and the silica surface; polyacrylamide (PAM) and polyvinyl alcohol (PVA). More clay could be coated over the silica sand using PVA than PAM. The clay-coated sand obtained by the PVA method was stable against pH variations between 3 to 11, whereas with the coated-sand obtained with the PAM method the clay was not stable and detached above pH 9. These two polymers did not cause a significant change in the electrophoretic mobilities of the minerals, however the wettability of illite and smectite decreased when interacting with the PVA.

Iron oxide-, clay-, and humic acid-coated sand permits to produce a porous material with similar hydraulic conductivity but different surface chemistry. The clay-coated sand caused anion exclusion during transport experiments. The hydrodynamic properties of the coated sand was evaluated using the Peclet number for each porous media. The Peclet numbers for all the porous media were similar.

The interaction between humic acids and clay minerals was studied in dynamic transport experiments, using clay-coated sand. Smectite, illite, and kaolinite were coated on silica sand using the PVA method. Humic acid breakthrough curve reached a maximum of 40% of the initial concentration in the illite- and smectite-coated sands.

Table of Contents

List of Tables

List of Figures

Chapter 1

Introduction

1.1 Background

Solute transport in the natural environment has been studied intensely in the last twenty years. Although column studies with natural porous media have provided valuable information, they have been criticized because they can not reproduce the variability of the natural environment. In addition, the presence of different mineral components and organic matter make it difficult to deduce mechanistic information from such studies. Column experiments using pure minerals can not reproduce all the interactions between the multiple components in the environment, but they can provide mechanistic information on solute interactions with the porous matrix.

The most reactive components in soils and sediments are aluminosilicate clays, iron and aluminum hydroxides, and humic materials. These components are small particles in the range of nanometers to micrometers; therefore, they are not suitable to be packed in a column to perform miscible transport experiments [*Wibulswas,* 2004]. Since the

mid 1960's scientists have developed method for coating different iron hydroxide on silica and quartz sand [*Chao and Harward*, 1964; *Kinniburgh et al.*, 1975; *Scheidegger et al.*, 1993]. These techniques have been used in combination with column experiments to study basic interactions of different solutes and iron minerals [*Stahl and James*, 1991; *Benjamin et al.*, 1996; *Gu et al.*, 1996a; *Hansen et al.*, 2001; *Hur and Schlautman*, 2003]. Similarly, humic acids have been immobilized on silica beads to determine the sorption coefficient (Koc) of pesticides [*Szabo et al.*, 1995; *Yang and Koopal*, 1999]. It would be very useful to immobilize aluminosilicate clays on an inert support, considering that clay cannot be packed into columns without significant hydraulic conductivity limitation.

1.2 Scope and Objective

The objective of this study was to develop a procedure to immobilize aluminosilicate clays on an inert silica support and to study the hydrodynamic properties of the modified silica sand. We coated silica grains with Georgia Kaolinite (KGa1), Texas Smectite (Stx1), and Morris Illite. Hydrodynamic properties of the coated silica sand media were tested with tracer experiments. Reactive transport experiments were conducted with humic acids.

1.3 Thesis Outline

The dissertation has three main chapters, two of which are papers submitted to peer-reviewed journals. Chapter 1 provides a brief overview and the objectives. Chapter 2 presents a new procedure to coat aluminosilicate clay on silica sand. This chapter describes the interaction of two polymers (polyacrylamide and polyvinyl alcohol) with three main aluminosilicate clays (Smectite, Illite, and Kaolinite) and silica sand. Chapter 3 describes the hydrodynamic properties of coated silica sand as a function of clay type and silica particle size. The surface properties of the porous medium were controlled with the coating of different minerals (aluminosilicate clays and ferrihydrite) and humic acid. The hydrodynamic properties were studied with tracer experiments. In Chapter 4, a review of humic-acid-clay interaction is presented, as well as transport experiments with humic acids. Chapter 5 gives the conclusions of the study.

Chapter 2

Coating of Silica Sand with Aluminosilicate Clay

2.1 Abstract

Aluminosilicate clays are important subsurface constituents, but are difficult to study in dynamic flow systems, because packed clays have inherently low hydraulic conductivity. The objective of this work was to immobilize aluminosilicate clays on an inert silica support, and to characterize the properties and stability of the clay-silica coating. Two polymers, polyacrylamide (PAM) and polyvinyl alcohol (PVA), were used to coat silica grains with kaolinite, illite, or smectite. Polymers acted as bridging agents between clay and silica surfaces. The clay-polymer interactions were studied by X-ray diffraction and electrophoretic mobility. Clay-coatings on silica grains were

This chapter has been submitted for publication: Jerez, J., M. Flury, J. Shang, and Y. Deng, Coating of Silica Sand with Aluminosilicate Clay. J. Colloid Interface Sci.

characterized by mass coverage, scanning electron microscopy, specific surface area, and pH stability. Silica sand was successfully coated with clays by using the two polymers, but with PVA, the clay coating had a greater mass coverage and was more stable against pH variations. Less polymer was needed for the clay coating using PVA as compared to PAM. Electrophoretic mobilities of the clay-polymer complexes were similar to the mobilities of the pure clay minerals, indicating that overall surface charge of the clays was little affected by the polymers. The methodology reported here allows to generate a clay-based porous matrix with hydraulic properties that can be varied by adjusting the grain size of the inert silica support.

2.2 Introduction

Clay minerals are important constituents of soils and sediments, and are used ubiquitously in industrial applications. Clay minerals can be used in environmental remediation and waste water treatment. For some of these applications, it would be desirable to pack clay minerals into columns and use the columns as filters or flow reactors. However, the use of clay minerals as filters or flow reactors is limited by the low hydraulic permeability of packed clay. In addition, possible compaction and clogging of pores due to migration of clay particles will further reduce the already low permeability. Clay minerals can be mixed with sand particles to increase hydraulic permeability, but clay particles can migrate and clog up pores [*Wibulswas*, 2004].

Alternative approaches have been proposed to overcome the limitation of the low

permeability. *Kocherginsky and Stucki* [2001] reported a procedure to immobilize clay minerals between two cellulose membranes to produce a clay filter membrane. Phillips and coworkers [*Ake et al.,* 2001*; Ake et al.,* 2003] developed a methodology to coat clay minerals onto inert silica grains. In this method, clay minerals are bound to silica surfaces by using natural polymers. The polymers are mixed with a solid support (silica sand or beads), and then clay minerals are added and thoroughly mixed. After drying and rinsing with water, a composite clay-silica material is obtained which can be used as a clay-based porous material [*Ake et al.,* 2001*; Ake et al.,* 2003]. Phillips and coworkers applied these clay-silica composites as flow through reactors to remove lead [*Ake et al.,* 2001] and organic contaminants [*Ake et al.,* 2003] from water.

Aluminosilicate clays are used in the production of ceramics. Porous ceramics have wide applications as insulators, filters, or suction devices. Clay-based ceramic pellets have been proposed as wastewater filters to remove contaminants such as Ni [*Márquez et al.,* 1991]. The high processing temperatures (600 to 1200°C) used for ceramic production, however, will change the surface properties of clay minerals. At temperatures of >600°C interlayers of 2:1 phyllosilicates collapse and kaolinite and illite transforms to mullite [*MacKenzie et al.,* 1996*; Hajjaji et al.,* 2002*; Aras,* 2004].

Materials like iron oxides and humic acids have been successfully attached to silica grains [*Scheidegger et al.,* 1993*; Yang and Koopal,* 1999]. Humic acid attachment to silica is facilitated through modification of the silica surface with aminosilane [*Vrancken et al.,* 1995]. Clay minerals can be attached to silica surfaces by using polymers as

binding agents [*Ake et al.*, 2001]. There is abundant information available on clay-polymer interactions [*Emerson*, 1963; *Heath and Tadros*, 1982; *Laird et al.*, 1992; *Mekhamer and Assaad*, 1999; *Bajpai and Vishwakarma*, 2003] as well as silica-polymer interactions [*Tadros*, 1978; *Argillier et al.*, 1996; *Stemme et al.*, 1999; *Stemme and Ödberg*, 1999; *Samoshina et al.*, 2003]. However, little is known about the use of polymers to bind clays onto silica surfaces. Phillips and coworkers proposed the use of mucilage and carboxymethylcellulose polymers to bind clay to silica surfaces [*Ake et al.*, 2001; *Ake et al.*, 2003]. Other polymers seem to be promising candidates for clay-silica bonding as well. One of these candidates is polyacrylamide (PAM), which is widely used in waste water treatment or erosion control as flocculant, because of its strong ability to bind clay minerals together. Polyacrylamide binds to clay surfaces via hydrogen bonding and ion exchange [*Laird et al.*, 1992]. Another promising polymer is polyvinyl alcohol (PVA), which was also used in erosion control [*Emerson*, 1963], and was found to have strong interactions with clay minerals [*Bajpai and Vishwakarma*, 2003; *Moen and Richardson*, 1984] while not affecting the cation exchange capacity of the clays [*Mekhamer and Assaad*, 1999].

Here, we propose to use PAM and PVA to bind clay minerals onto silica surfaces to produce a composite clay-silica material. Our objective was to develop an experimental methodology to bind aluminosilicate clays onto silica particles and to systematically test the homogeneity of the surface coverage and the stability of the clay-silica composites. The clay-silica composite can be packed into flow-through columns or reactors

that are dominated by clay mineral surfaces, yet have the hydraulic properties of the inert silica support. Such a porous composite can be used to study interactions between chemicals and clay surfaces in dynamic flow experiments, and can possibly be applied as reactive filters for environmental remediation.

2.3 Materials and Methods

2.3.1 Silica Sand, Aluminosilicate Clay Minerals, and Polymers

Silica sand was obtained from J.T. Baker, Inc. (Phillipsburg, NJ; CAS No. 14808-60-7), and dry sieved to fractionate particles between 0.25 mm and 0.5 mm diameter. Organic matter was removed with H_2O_2 [*Kunze and Dixon,* 1986] and iron oxides with the citrate-dithionite method [*Holmgren,* 1967]. After these treatments, the sand was thoroughly washed with deionized water and oven dried at 110°C.

Texas smectite (STx1) and Georgia kaolinite (KGa1) were obtained from the Clay Minerals Repository (University of Missouri). Illite (No. 36, Morris, Illinois) was obtained from Ward's Natural Science (Rochester, NY). All clays, as received from the suppliers, were pretreated to remove organic matter with H_2O_2 [*Kunze and Dixon,* 1986] and iron oxides with the citrate-dithionite method [*Holmgren,* 1967]. The pretreated clays were then fractionated by gravity sedimentation to obtain minerals smaller than 2 μm in diameter, repeated two to three times. Then the clays were

made homoionic by washing with 0.5 M $CaCl_2$, 1 M NaCl, or 1 M KCl to obtain Ca-smectite, Na-kaolinite, and K-illite [*van Olphen,* 1977]. Finally, the clays were dialyzed with deionized water until the electrical conductivity of the dialysate was less than 5 μS/m.

2.3.2 Interactions of Polymers with Aluminosilicate Clays

We determined sorption isotherms for both PAM and PVA on smectite, kaolinite, and illite. Clay suspensions were equilibrated with a series of polymer concentrations. Specifically, 0.2 g of clay were equilibrated with 20 ml polymer solution of various concentrations at the same pH used in the coating procedure. For PAM, the pH was 7 and the polymer concentrations ranged from 0 to 150 mg/L; for PVA, the pH was 5 and the concentrations ranged from 0 to 300 mg/L. The polymer-clay suspension was then agitated on a reciprocal shaker for 24 h at room temperature and then the suspensions were centrifuged at 10,000 g for 15 min. The polymer concentrations in the liquid phase were determined by UV/VIS spectrometry (HP 8452A, Hewlett-Packard) at wavelengths of 200 nm for PAM and 190 nm for PVA. The amount of polymer sorbed onto the clay was calculated using the mass balance method.

To check for mineralogical alterations of smectite due to polymer sorption we determined X-ray diffraction (XRD) patterns for smectites containing different amounts of polymers. The XRD was performed with Cu-K radiation (Philips XRG 3100, Philips Analytical Inc., Mahwah NJ) and with scanning rates of $0.02^o\theta$/sec.

2.3.3 Coating of Silica Sands with Aluminosilicate Clays

To coat silica grains with clay minerals, we followed the general approach proposed by Phillips and coworkers [*Ake et al.,* 2001*; Ake et al.,* 2003]; however, we used different polymers and a different sequence of mixing the sand, clays, and polymers. We used two procedures to coat silica grains with clay minerals, using two different polymers.

The first procedure employed a cationic PAM (Superfloc C498, Cytec Industries, West Paterson, NJ), which, according to the manufacturer, has a molecular weight of ≈5000 kg/mol and 55% of cationic N,N,N-trimethyl aminoethylacrylate units. Clay suspensions (≈4 g/L particle concentration) were flocculated with PAM at various pH and PAM concentrations. The mixture was left to settle for about 3 h at room temperature and then centrifuged at 100 g for five minutes. The clay-polymer complex was separated from the bulk solution by decanting the supernatant and was then mixed with the silica sand to produce a slurry. The sand-clay-polymer slurry was placed on a reciprocal shaker over night. The clay-to-sand ratio was 1:20 (w/w). Finally, the coated sand was dried at 100°C for 24 h. After drying, the sand was washed with deionized water to remove loose particles and dried again at 100°C for 24 h.

To optimize the methodology, we tested the effects of pH and PAM concentration during clay flocculation. The pH effect was tested at a polymer concentration of 50 mg/L where the pH was varied between 3 and 11 using NaOH or HCl. The effect of the polymer concentration was tested at pH 7 where PAM concentrations were varied between 25 and 150 mg/L (≈5 and 30 nmol/L). We also tested the effect of the

clay-to-sand ratio (w/w) at pH 7 and 50 mg/L PAM.

The second procedure employed a non-ionic polyvinyl alcohol (Lot# 386921/1, Fluka, Switzerland), which has a molecular weight of 200 kg/mol, and a 98% degree of polymerization. Clay suspensions at a concentration ≈40 g/L were mixed with PVA and agitated manually for about 30 minutes, after which the silica sand was added to the suspensions, and the mixture was stirred with a perforated Teflon stirrer for a few minutes. The mixture was then dried at 80°C for 24 hour. After drying, the sand was washed with deionized water and dried again at 80°C for 24 hour.

This procedure was optimized by adjusting pH and PVA concentration as described above for PAM. The only differences were that the effect of the polymer concentration was tested at pH 5, and the PVA concentrations ranged from 20 to 200 mg/L (≈100 to 1000 nmol/L). We also tested the effect of the clay-to-sand ratio (w/w) at pH 5 and 80 mg/L PVA. We consider that the optimal pH and polymer concentration were those that produced the greatest amount of clay coating. The amount of clay coating was determined as described below. For PAM, the optimal pH was 7 and polymer concentration was 50 mg/L; for PVA, the optimal pH was 5 and polymer concentration was 80 mg/L.

2.3.4 Characterization of Coated Silica Sands

The amount of clay coated on the silica grains was determined by detaching and measuring the amount of detached clay. For PAM, clays were detached by immersing

the coated silica sand in a non-stirred pH 13 solution (adjusted with NaOH) for 24 h. For PVA, clays were detached by immersing the coated silica sand in a pH 7 solution and sonicating six times for 45 minutes in intervals of 3 to 4 hours. These procedures removed the clay coating effectively, as verified by microscopy. The amount of detached clay was quantified by UV/VIS spectrometry for PAM, and by gravimetry for PVA.

Further characterization of the coated sands was only performed on the samples found to have the optimal (greatest) amount of clay coating. We examined morphology and uniformity of the coating, the specific surface area, the stability of the coating, and selected surface properties of the coated sands. The morphology of the coated sand particles was examined by scanning electron microscopy (Hitachi S520). Specific surface areas were determined on oven dried samples by N_2 adsorption and fitting a BET isotherm (ASAP2010, Micromeritics, Norcross, GA). We measured the surface areas of both the aluminosilicate source clays as well as the clay-coated sands.

The stability of the coating was evaluated by immersing the coated sand into solution of different pH, ranging from pH 3 to 13, adjusted with NaOH or HCl. We placed 0.3 to 0.5 g of coated sand and 18 mL of solution at a specific pH into 20 mL glass vials, which were then capped. The vials were kept non-stirred at room temperature. Aliquots of 3.5 mL were sampled from each vial after intervals of 1 hour, 1 day, and 1 week. Before the aliquots were taken, the vials were rigorously shaken to suspend the detached clay particles. The suspended clay was then quantified by UV/VIS spectrometry at wavelengths of 230 nm for kaolinite and smectite and 256 nm

for illite. The sample volume was replaced with fresh solution of the specific pH.

The stability was also assessed with long-term column experiments (Figure 2.2) . Clay-coated sand was packed into chromatography columns (i.d. 0.7 cm, length 12 cm) (Kontes Flex column, with a 20 μm frit at the bottom), and a downward steady-state flow using deionized water adjusted to pH 8 was established. The flow rate was 12 mL/h, corresponding to a pore water velocity of 70 cm/h. A total of 5,000 pore volumes was passed through the column. Column outflow was periodically checked for the presence of suspended particles using light scattering (ZetaSizer 3000 HSA, Malvern Instruments Ltd., Malvern, UK). The amount of clay coated on the sand was determined at the beginning and at the end of the column experiment by the methodology described previously. At the end of the experiment, the column was emptied and the clay content remaining on the sand determined.

2.3.5 Electrophoretic Mobility and Contact Angle Measurement

Electrophoretic mobility and surface thermodynamic properties were determined on the pure and polymer-treated clay minerals rather than the coated sands themselves. Electrophoretic mobility was determined by dynamic light scattering in a 10 mM NaCl solution (ZetaSizer 3000 HSA, Malvern Instruments Ltd., Malvern, UK). The measurements were made over a pH range from 3 to 11, adjusted overnight with HCl or NaOH.

Contact angle of the clays was measured by the sessile drop method using a goniometer (Ramé-hart, model 50-00-115, Mountain Lakes, NJ). Thin films were prepared by the solvent evaporation method. Clay minerals (diameter <2 μm) at a concentration of 20 g/L were dispersed in double distilled water, shaken on a reciprocal shaker for 30 min, and then sonicated for 10 min. The particles were kept in suspension by continuous stirring with a magnetic stirrer. An aliquot of 5 mL was withdrawn with a pipette and distributed evenly on a microscope slide, which was kept strictly horizontal. The suspension was evaporated at room temperature (20°C). Clay-polymer films were prepared using the same clay-polymer ratio and pH used for the best clay coating procedure. Pure polymer films were made from a solution of 10 g/L, and the polymer solution was evaporated at room temperature (20°C).

The films on the microscope slides were used for contact angle measurement. The liquid was dropped with a glass syringe and a stainless steel needle. The size and volume of the drops were kept constant (about 5 mm diameter and 12$\pm$2 μL) as variation in the volume can lead to inconsistent measurements [*Marmur,* 1998]. The contact angle was measured within 10 to 15 s. A total of 15 to 18 drops were measured for each clay sample and test liquid. We used water, diiodomethane, formamide, glycerol, and ethylene glycol as test liquids.

2.3.6 Clay and Clay-polymers Surface Thermodynamics

The measured contact angles were used to calculate the surface free energies. The surface tension (γ_i) is the sum of two components, the Lifshitz-van der Waals (γ_i^{LW}) and the acid-base component of the surface tension (γ_i^{AB}) [*van Oss*, 1994]:

$$\gamma_i = \gamma_i^{LW} + \gamma_i^{AB} \tag{2.1}$$

and γ_i^{AB} is

$$\gamma_i^{AB} = 2\sqrt{\gamma_i^+ \gamma_i^-} \tag{2.2}$$

where γ_i^- is the electron-donor and γ_i^+ is the electron-acceptor component of the surface tension, and the subscript i denotes solid ($i = S$) or liquid ($i = L$).

The total free energy of solid-liquid adhesion (ΔG_{SLS}^{TOT}), according to the theory of van Oss, Chaudhury, and Good can be determined by [*van Oss*, 1994]:

$$\Delta G_{SLS}^{TOT} = \Delta G_{SLS}^{LW} + \Delta G_{SLS}^{AB} \tag{2.3}$$

where ΔG_{SLS}^{LW} is the Lifshitz-van der Waals component and ΔG_{SLS}^{AB} is the acid base component of the free energy, which can determined by:

$$\Delta G_{SLS}^{LW} = -2\left(\sqrt{\gamma_S^{LW}} - \sqrt{\gamma_L^{LW}}\right)^2 \tag{2.4}$$

$$\Delta G_{SLS}^{AB} = -4\left(\sqrt{\gamma_S^- \gamma_S^+} + \sqrt{\gamma_L^- \gamma_L^+} - \sqrt{\gamma_S^+ \gamma_L^-} - \sqrt{\gamma_S^- \gamma_L^+}\right) \tag{2.5}$$

The components of the solid surface tension (γ_S^+, γ_S^-, and γ_S^{LW}) can be obtained by measuring the contact angles of liquids of known surface tension components, and

solving the Young-Dupré equation [*van Oss,* 1994]:

$$(1 + \cos\theta)\gamma_L = 2\left(\sqrt{\gamma_S^{LW}\gamma_L^{LW}} + \sqrt{\gamma_S^+\gamma_L^-} + \sqrt{\gamma_S^-\gamma_L^+}\right) \tag{2.6}$$

We used the contact angles of water, diiodomethane, formamide, glycerol, and ethylene glycol to determine the unknown components of the surface tension $\gamma_S^{LW}, \gamma_S^+$, and γ_S^- using non-linear least-squares.

To evaluate whether the surface is monopolar, we can calculate the polarity ratios [*van Oss,* 1994*; Faibish et al.,* 2001]

$$\delta_i^- = \sqrt{\gamma_i^-/\gamma_w^-} \quad \text{and} \quad \delta_i^+ = \sqrt{\gamma_i^+/\gamma_w^+} \tag{2.7}$$

where δ_i^- is the relative Lewis acid and δ_i^+ is the relative Lewis base polarity of a substance i with respect to water w ($\gamma_w^+ = \gamma_w^- = 25.5$ mJ/m^2). If $\delta_i^- \ll 0.2$ or $\delta_i^+ \ll 0.2$, then the surface is considered monopolar [*van Oss,* 1994].

2.4 Results and Discussion

2.4.1 Interactions of Polymers with Aluminosilicate Clays

The aluminosilicate clays had a high affinity to sorb PAM and PVA. The adsorption isotherms (Figure 2.3) were similar to the ones previously reported for PAM [*Argillier et al.,* 1996] and PVA [*Emerson,* 1963*; Greenland,* 1963*; de Bussetti and Ferreiro,* 2004]. Both polymers presented a high affinity to the aluminosilicate clays, however PVA adsortion was greater than PAM. The PAM adsorption reached a maximum of

about 42, 30, and 8 mg of polymer per gram of clay for smectite, illite, and kaolinite respectively. PAM adsorption on smectite reached a maximum at about 60 mg/l after which the adsorption decreased consistently. This may be explained by the high coagulation capacity of the polymer, which creates clusters that prevent some of the clay to be in contact with the polymer. For PVA, the maximum was only reached for kaolinite, the maximum adsorption on the others was not reached in the concentration range studied. In general, the interaction of polymers with clays depends on the polymer access to the clay surfaces [*Theng,* 1979]. As was previously demonstrated [*Greenland,* 1963], the amount of polymer sorption decreases as the clay concentration increases. This is because polymers cause clay aggregation, which in turn reduces available surface areas for polymer sorption [*Greenland,* 1963]. In our experiments (data not shown) this phenomenon was more pronounced for PAM than for PVA. For PAM, clay concentrations greater than 4 g/L reduced polymer sorption, while for PVA, clay concentrations up to 40 g/L did not reduce polymer sorption.

X-ray diffraction patterns at 300°C for different polymer loadings on smectite clay are shown in Figure 2.4. All diffraction patterns collected at room temperature were identical, independent of polymer loading, and were identical to the pattern of the pure clay. Upon heating to 300°C, smectite interlayers usually collapse from d-spacing 1.4 nm to 1 nm, as shown in Figure 2.4 for the pure smectite. However, when the smectite was treated with polymers, the interlayer did not collapse anymore, and this phenomenon became more pronounced at higher polymer loadings. This suggests that

the polymers accessed the clay interlayers, and prevented its collapse upon heating.

2.4.2 Optimization of Experimental Parameters for Clay-coating of Silica Sand

The effect of pH during the coating procedure on the amount of clay coated on the silica sand is shown in Figure 2.5. For PAM, the greatest amount of coating was achieved at pH≈7, whereas for PVA, the optimal coating was achieved at pH≈5. The existence of an optimal pH may be explained as follows. For PAM, increasing the pH enhances polymer-clay interaction [*Theng,* 1979*; Deng,* 2001]; however, the polymer-silica interaction becomes unstable as the pH increases above pH 8 (see discussion on polymer-silica stability below). For PVA, the interaction with both, clay minerals and silica surfaces, is strongest at low pH [*Tadros,* 1978*; Theng,* 1979]. At low pH, however, clays are poorly dispersed and consequently difficult to mix with polymers. These mechanisms result in a decreased clay-coating at low or high pH, while the optimal pH is about 5.

The effect of polymer concentration used in the coating procedure on the amount of clay coating is illustrated in Figure 2.6. As the polymer concentrations were increased, the amount of clay coating initially increased. However, after the polymer exceeded a certain concentration, the clay coating decreased. For PAM, the optimal polymer concentration was about 50 mg/L and for PVA 80 mg/L. For PAM concentrations >100 mg/L, a clear reduction on the amount of clay coating was observed. This

reduction is likely caused by flocculation induced by the PAM that hindered clay-polymer interactions [*Theng,* 1979]. This behavior was observed for PVA as well, but was not as pronounced.

The effect of the clay-to-sand ratio on the amount of clay coated is summarized in Table 2.1. For PAM, the increase in the clay-to-sand ratio did not increase the amount of clay coated on the sand surface, except for kaolinite. On the contrary, an increase of the clay-to-sand ratio in the PVA method resulted in greater clay-coating.

The experimental conditions that were considered optimal for the clay coating, i.e., greatest amount of clay coated onto the silica surface, were used to produce a batch of coated sand. The optimal conditions are summarized in Table 2.2. For these optimal coating conditions, the concentrations of the polymers on the clays are in the order of a few milligrams polymer per gram of clay (Table 2.3). The optimally-coated sand was characterized in detail and the results are described below.

2.4.3 Characterization of Coated Silica Sands

The specific surface areas of the pure minerals used and the clay-coated sands are listed in Table 2.4. The surface areas of the coated sand ranged from 0.24 to 2.5 m^2/g. These values are one to two orders of magnitude larger than that of the uncoated silica sand. The PVA method produced much larger surface areas than did the PAM method.

The amount of clay coated onto the silica surface followed the trend observed with

the specific surface areas (Table 2.4). Specifically, a much larger amount of coating was observed for PVA than for PAM. The considerable difference between PAM and PVA coatings is highlighted by calculating the amount of clay per surface area of the silica support. The PVA method produced a clay coverage of about 2000 mg/m^2, which is 3 to 10 times larger than the coverage obtained by the PAM method.

Scanning electron micrographs of clean and clay-coated sands are shown in Figure 2.7. The uncoated silica surface had an irregular topography (Figure 2.7a). In the micrographs of the clay-coated sands, the clays can be readily identified with morphologies similar to the ones reported in the literature [*Murray,* 2000]. The individual clay particles were smaller than 2 μm. The clays covered $\approx$70 to 80% of the sand surface with a non-uniform distribution. The micrographs show areas with no clay coating next to areas with high clay coating. The non clay-coating areas appeared to coincide with smooth topography of the silica surface. This was particularly evident for the PAM coating methodology (Figure 2.7b and f). The PVA methodology resulted in multilayer clay coating, with coatings up to 25 μm thick (Figure 2.7g, insert). The clay coating also created microporous structures on the silica sand surface (Figure 2.7c,e).

The pH stability of the clay coating is illustrated by plotting the amount of clay attached to the silica surface as a function of pH after a specific time (Figure 2.8). The clay-coating used in the PAM methodology was not stable at high pH; at pH $>$ 9, the clay detached from the sand (Figure 2.8, left panels). We attribute the instability of

the clay-PAM-silica bonding to a weakening of the polymer-silica bonding, because we expect the polymer-clay coating to be stable at high pH [*Deng,* 2001]. The stability of the clay coating was not affected by time for up to one week, except at high pH, where we observed increased clay detachment with increasing time.

The PVA coatings were stable over the entire pH range investigated (Figure 2.8, right panels). The stability of the clay coating was not affected by time for up to one week. The strong pH independent bonding between clay-PVA-silica is likely due to H-bonding between the hydroxyl groups of the PVA and the basal oxygen of the clay, which is independent of pH [*Emerson,* 1963*; Emerson and Raupach,* 1964].

The results of the long-term stability experiment are presented in Table 2.5. The clay-coated sand with the PAM method had poor long-term stability, only between 17.8 and 35.8% of the initial clay remained on the sand after 5,000 pore volume. On the contrary, the clay-coated sand using the PVA method was stable, around 97% of the initial clay remained on the sand. The light scattering data from the column never showed above-background scattering, suggesting that the clay was removed in concentrations below the limit of detection of the instrument.

2.4.4 Surface Thermodynamic Properties

By and large, the polymers did not affect the electrophoretic mobility of the clay minerals (Figure 2.9). Electrophoretic mobilities of pure smectite was constant over the pH range from 3 to 12, corroborating results reported by others [*Thomas et al.,*

1999]. Electrophoretic mobilities of illite and pure kaolinite were pH dependent. The results of pure kaolinite are similar to those reported by others [*Kretzschmar et al.*, 1998]; for illite we could not find any published data.

It was reported that clay-PAM complexes have about 70% of the original clay cationic exchange capacity (CEC) [*Deng,* 2001], and that clay-PVA complexes have the same CEC as the original clay minerals [*Mekhamer and Assaad,* 1999*; Theng,* 1979*; Emerson and Raupach,* 1964].

The results of the contact angle measurement are summarized in Table 2.6. The values for smectite agree with previously reported data [*Wu,* 2001]. Different values of contact angles of kaolinite have been reported: 46.1^o was obtained with thin-layer wicking [*Wu,* 2001] and about 4^o was obtained with a goniometer method similar to ours [*Gu et al.*, 2003]. Our values compare well with the previosuly reported goniometer values.

Both kaolinite and illite did not produce smooth surfaces on the glass slides, and the goniometer measurements may not be accurate; however, the measurements were reproducible. Although the absolute value of the contact angles for kaolinite and illite may have to be considered with caution, we can interpret the relative differences between pure and polymer-coated clays.

The water-contact angle of PVA is in agreement with reported values for PVA of similar molecular weight [*Nguyen,* 1996]. The wettability of the clay minerals and the clay-polymer complexes can be analyzed by comparing the contact angles obtained for

the surface-water and surface-diiodomethane (DIM) interface, as these two solvents are reference liquids for polar and apolar solvents [*Faibish et al.,* 2001]. The contact angles of the polymer-films, in both solvents, are greater than the contact angles of the clay minerals, indicating that the polymers have less hydrophilic surface. By and large, the clay-polymer complexes had greater water contact angles than pure clay minerals. The most significant effect of PAM was observed on illite, where the water contact angle was doubled after addition of PAM. A similar pattern was observed for the illite-PVA complex, but the change in the water-contact angle was less pronounced (+ 58%). This indicates that the two polymers considerably reduced the wettability of illite. Similarly, the polymers also increased the DIM-contact angle of the illite-polymer complexes. The smectite-polymer complexes had smaller DIM-contact angles than the smectite itself. No clear trend in water and DIM-contact angle were obvious for kaolinite.

The surface tensions and free energies are shown in Table 2.7. The values of the surface tension and free energy components for smectite and kaolinite were similar to those reported previously [*Wu,* 2001]. The effect of the polymer on the surface tension components (γ_S^{LW}, γ_S^+, and γ_S^-) did not reveal a clear trend for any of the clay minerals. For smectite, PVA coating resulted in a 20% reduction of ΔG_{SLS}^{TOT}, but PAM did not cause any considerable change in the total surface-free energy. For illite, the coatings of the polymers caused considerable change in surface tension and free energy. The largest change was observed in the electron-acceptor component (γ_S^+) which was

twice as large for the clay-polymer complex than the clay itself. We also observed a reduction in the electron donor component (γ_S^-) of 31% for illite-PAM and 16% for illite-PVA complexes. This resulted in a considerable reduction of ΔG_{SLS}^{TOT}: 70% for illite-PAM and 34% for the illite-PVA complex. The surface tension and surface free energy of kaolinite were not affected by the polymer coating. The addition of the polymers caused little change in wettability of the clay minerals except for illite-PAM, illite-PVA, and smectite-PVA composite. The polarity ratio showed that the clays were monopolar, and the addition of the polymers did not change the polarity ratio.

2.5 Conclusions

We developed a successful method to coat inert silica support with aluminosilicate clays. The clay was attached to the silica surface via a polymer bonding. At the polymer concentration used, the polymers PAM and PVA, did not significantly affect the electrophoretic mobility of the clay minerals. A greater amount of clay could be attached to silica by using PVA as compared to PAM. The PVA method produced clay coatings that were stable in aqueous solution over the pH range of 3 to 11, whereas the PAM method showed reduced attachment stability above pH 9.

The PAM and PVA reduced the wettability of illite, and PVA reduced the wettability of smectite. The surface properties of kaolinite were not affected by the polymers. The monopolarity of the clay minerals was not affected by the polymers.

The potential to produce a porous medium with high hydraulic conductivity, but

with surfaces controlled by clay minerals, allows to study clay-solute interactions in dynamic flow systems. Dynamic flow systems have several advantages over batch systems, and are often more representative of natural subsurface conditions. Clay-coated sand also has potential applications in environmental remediation, where the porous clay structure can be used as reactive filter. For such applications, the long-term stability of the clay coatings under conditions expected at remediation sites would need to be investigated.

2.6 Tables and Figures

Table 2.1: Amount of clay coated on silica sand (mg clay/ g sand) for different clay-to-sand-ratio.

Clay Minerals	Initial Clay-to-sand Ratio (g clay/g sand)		
	1:10	1:20	1:40
Polyacrylamide (PAM)			
Smectite (STx1)	2.9±0.2[b]	3.1± 0.3	2.1 ±0.1
Illite (No. 36, Morris)	4.8±0.50	5.0±0.1	4.3 ±0.2
Kaolinite (KGa1)	22.1±1.3	24.7±0.9	10.1 ±1.1
Polyvinyl Alcohol (PVA)			
Smectite (STx1)	67±5	29 ±1	15±2
Illite (No. 36, Morris)	77±3	32 ±3	18±1
Kaolinite (KGa1)	88±6	61 ±5	23±2

[b] error bar are one standard deviation.

Table 2.2: Experimental conditions for optimal (greatest) clay coating on silica sand.

Experimental Parameter	Value/Condition
Polyacrylamide (PAM)	
pH	7
PAM concentration	50 mg/L
Clay suspension concentration	4 g/L
Clay-to-sand ratio	1:20 w/w
Polyvinyl Alcohol (PVA)	
pH	5
PVA concentration	80 mg/L
Clay suspension concentration	40 g/L
Clay-to-sand ratio	1:10 w/w

Table 2.3: Amount of polymer sorbed per gram of clay for the case of optimal (greatest) clay coating.

Clay Minerals	Polyacrylamide (mg/g)	Polyvinyl Alcohol (mg/g)
Smectite (STx1)	10	1.9
Illite (No. 36, Morris)	9	1.9
Kaolinite (KGa1)	5	1.3

Table 2.4: Characterization of minerals and coated sand.

Material	Specific Surface Area BET (m^2/g)	Amount of Clay Coating (mg/g)	(mg/m^2)[a]
Pure minerals			
Uncoated Sand	0.04±0.001[b]	none	none
Smectite (STx1)	52.6±0.9	none	none
Illite (No. 36, Morris)	36.5±0.4	none	none
Kaolinite (KGa1)	13.6±0.3	none	none
Coated sands with PAM methodology			
Smectite (STx1)	0.35±0.01	3.1±1.4	77
Illite (No. 36, Morris)	0.29±0.01	5.0±0.4	126
Kaolinite (KGa1)	0.24±0.01	24.7±3.1	618
Coated sands with PVA methodology			
Smectite (STx1)	2.41±0.03	67±5	1673
Illite (No. 36, Morris)	2.49±0.05	77±5	1920
Kaolinite (KGa1)	0.54±0.01	88±6	2205

[a] calculated from the amount of clay coating (mg/g) divided by the specific surface area of clean sand.

[b] error bar are one standard deviation.

Table 2.5: Amount of clay remaining on the sand surface after 5.000 pore volume leaching experiment.

Clay Minerals	Initial Amount of Clay Coating (mg/g)	Final Amount of Clay Coating (mg/g)	Final Amount of Clay Coating (% of initial)
Polyacrylamide (PAM)			
Smectite (STx1)	3.5±0.4[a]	1.25±0.06	35.7
Illite (No. 36, Morris)	4.8±0.7	0.82±0.06	17.1
Kaolinite (KGa1)	18.3±1.2	4.17±0.18	22.8
Polyvinyl Alcohol (PVA)			
Smectite (STx1)	16.7±2.1	16.3±1.1	97.6
Illite (No. 36, Morris)	25.6±3.2	24.8±0.38	96.9
Kaolinite (KGa1)	22.3±1.9	21.9±0.60	98.2

[a] error bar are one standard deviation.

Table 2.6: Liquid-solid contact angle (degree) of clays and clay-polymer complexes.

	Water	Glycerol	Formamide	Diiodomethane	Ethylene Glycol
			Smectite		
STx1	20.1±1.7[a]	28.2±1.3	8.9±1.0	31.5±1.1	18.3±0.9
STx1 + PAM	16.5±2.0	22.5±2.6	7.1±1.2	26.1±1.9	8.2±2.2
STx1 + PVA	22.8±1.6	23.4±2.3	10.3±1.8	25.8±1.5	13.3±2.3
			Illite		
Illite	18.1±1.0	26.0±1.2	12.9±1.4	30.3±1.7	15.4±1.5
Illite + PAM	36.4±2.4	30.3±2.8	18.8±2.0	32.6±2.1	15.5±2.2
Illite + PVA	28.6±2.6	28.6±2.2	15.6±1.6	37.5±1.8	16.3±2.5
			Kaolinite		
KGa1	7.7±0.8	27.3±1.4	12.1±0.9	23.4±1.3	20.6±1.7
KGa1 + PAM	10.4±0.7	31.7±1.5	14.2±1.3	20.3±1.2	18.1±1.4
KGa1 + PVA	16.7±2.2	34.1±3.7	22.6±4.9	24.7±1.5	20.7±3.1
			Polymers		
PAM	71.5± 1.1	56.4±3.1	51.0±8.4	48.9±1.7	67.5±4.9
PVA	73.4± 1.8	60.3±1.3	32.3±0.9	42.1±1.0	32.3±1.2

[a] errors are one standard deviation.

Table 2.7: Surface tension,γ, surface-free energy, ΔG (mJ/m^2), and polarity ratios, δ^- and δ^+, of clay and clay-polymer complexes.

	γ_S^{LW}	γ_S^+	γ_S^-	ΔG_{SLS}^{LW}	ΔG_{SLS}^{AB}	ΔG_{SLS}^{TOT}	δ^-	δ^+
	Smectite							
STx1	45.8±0.4[a]	0.42±0.02	53.0±0.9	−8.8±1.2	39.3±0.3	30.5±0.9	0.13	1.44
STx1 + PAM	43.9±0.6	0.42±0.01	52.8±0.7	−7.7±0.9	39.0±0.4	31.4±0.5	0.13	1.44
STx1 + PVA	45.9±0.5	0.45±0.01	48.8±0.6	−8.9±0.8	33.9±0.3	25.0±0.5	0.13	1.38
	Illite							
Illite	44.2±0.7	0.41±0.07	53.8±0.1	−7.8±0.5	40.3±0.4	32.5±0.1	0.13	1.45
Illite + PAM	43.2±0.8	0.82±0.04	37.1±1.8	−7.2±2.5	17.3±0.5	10.0±2.1	0.18	1.21
Illite + PVA	41.0±0.8	0.87±0.05	45.2±1.7	−6.0±2.3	27.6±0.4	21.5±1.8	0.18	1.33
	Kaolinite							
KGa1	46.8±0.5	0.11±0.01	60.2±0.3	−9.5±0.5	51.1±0.3	41.7±0.8	0.07	1.54
KGa1 + PAM	47.9±0.3	0.05±0.01	59.8±0.4	−10.1±0.8	51.8±0.2	41.7±1.0	0.04	1.53
KGa1 + PVA	46.3±0.4	0.05±0.05	58.4±1.3	−9.1±3.3	50.0±0.2	40.9±3.1	0.04	1.51

[a] errors are one standard deviation.

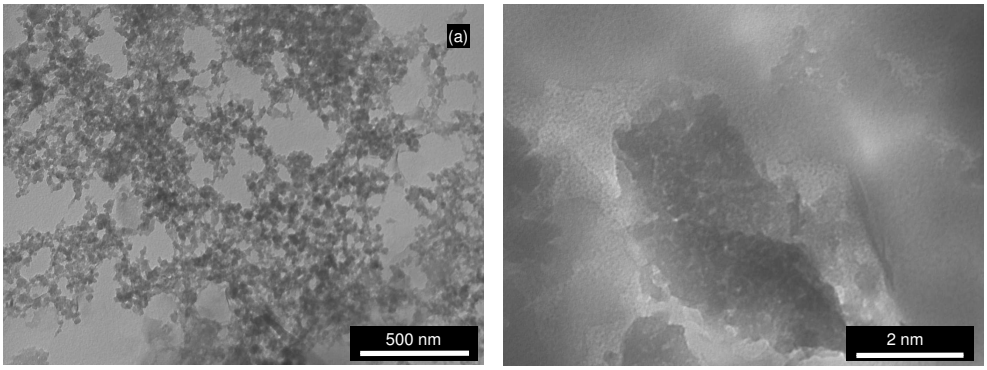

Figure 2.1: Transmission Electron Micrograph of polymers. (a) Polyacrylamide, (b) Polyvinyl alcohol.

Figure 2.2: Pictures of the long-term stability experiments

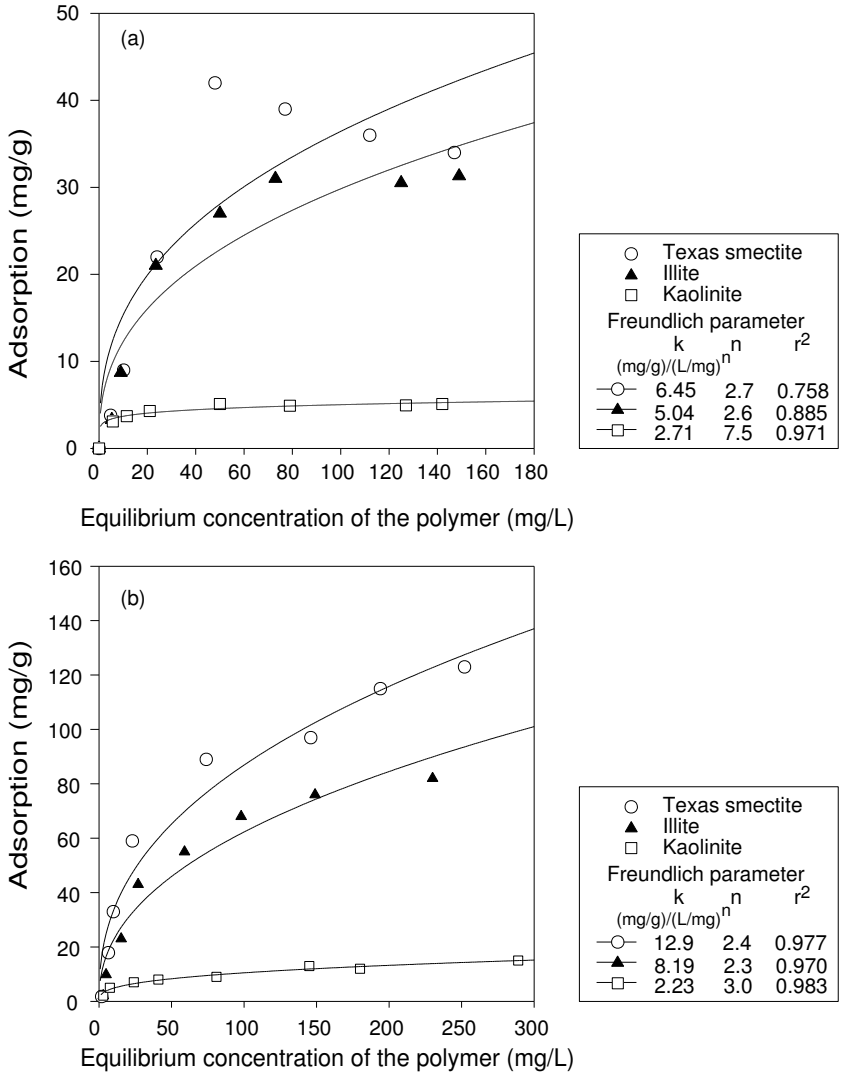

Figure 2.3: Adsorption isotherms of (a) Polyacrylamide (PAM) and (b) Polyvinyl alcohol (PVA) on smectite, illite, and kaolinite.

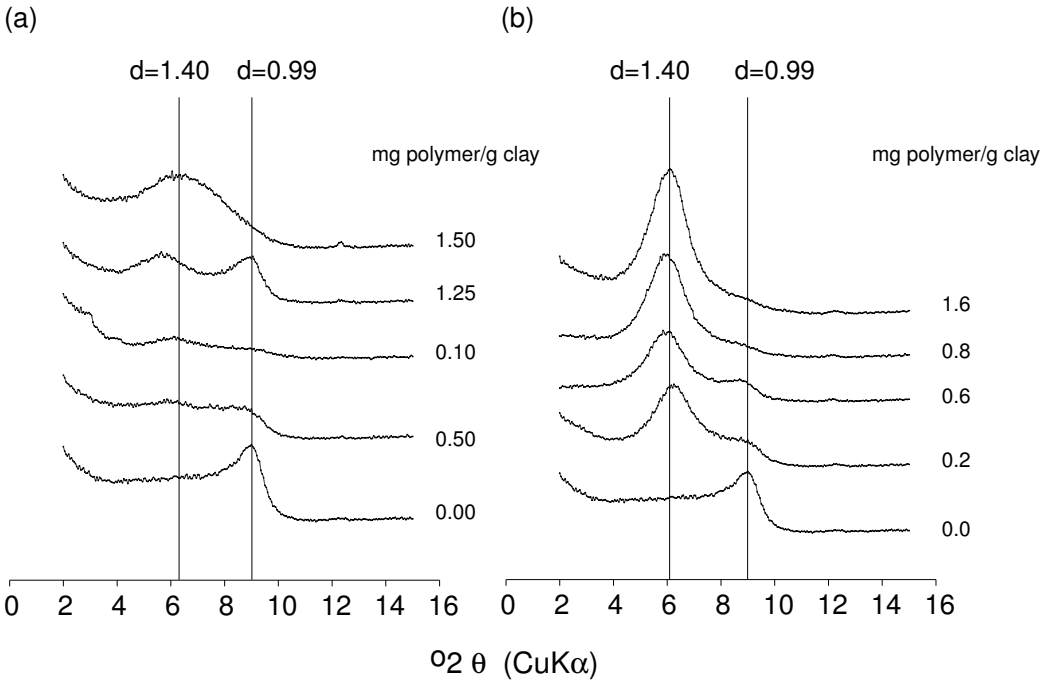

Figure 2.4: X-ray diffraction patterns of smectite (STx1) treated with (a) PAM and (b) PVA heated to 300°C.

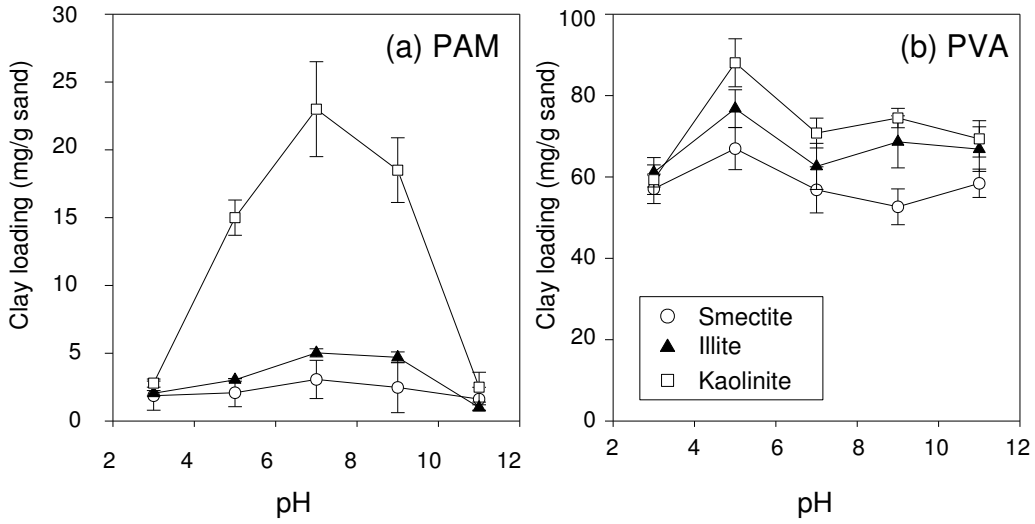

Figure 2.5: Effect of pH on clay coating of silica sands using (a) polyacrylamide (PAM) and (b) polyvinyl alcohol (PVA) for different clay minerals. Error bars denote one standard deviation of three repetitions.

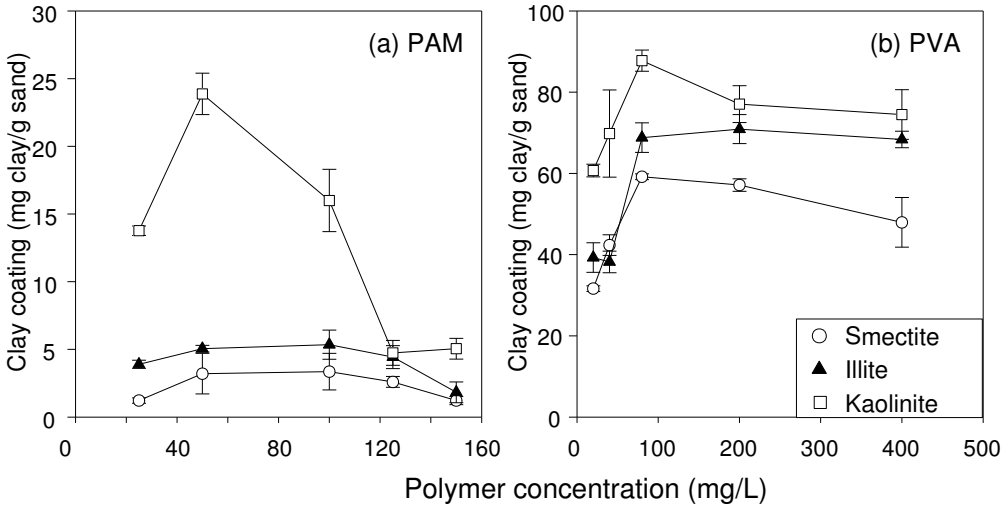

Figure 2.6: Effect of polymer concentration on clay coating for (a) polyacrylamide (PAM) at pH 7, and (b) polyvinyl alcohol (PVA) at pH 5. Error bars denote one standard deviation of three repetitions.

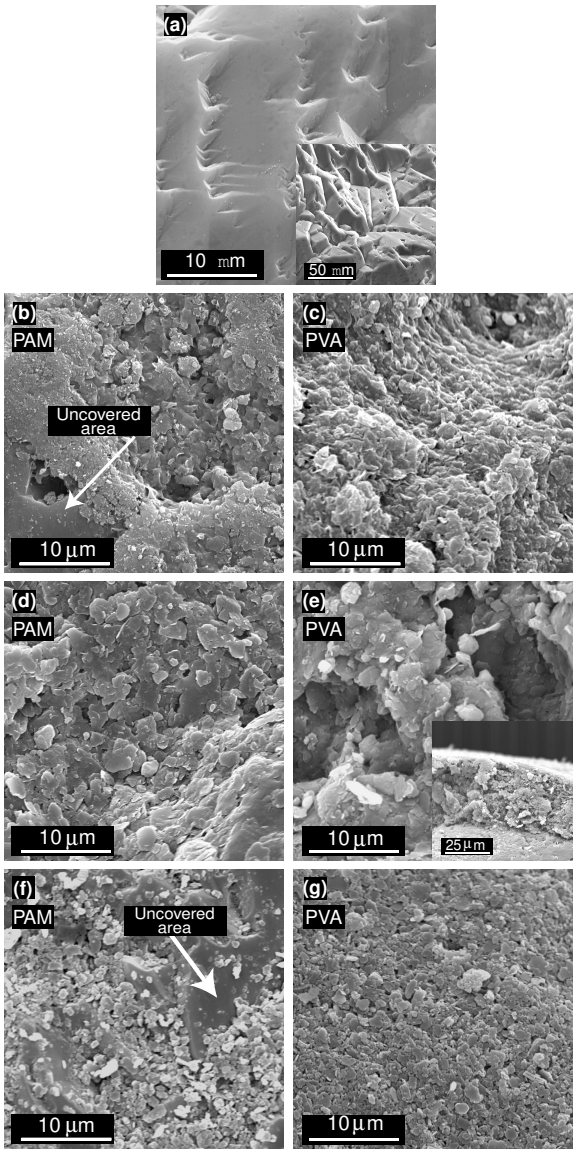

Figure 2.7: Scanning electron micrographs of (a) uncoated silica sand, (b,c) smectite-coated sand, (d,e) illite-coated sand, and (f,g) kaolinite-coated sand. The left column (b,d,f) shows sand coated with the polyacrylamide (PAM) method, the right column (d,e,g) shows sand coated with the polyvinyl alcohol (PVA) method.

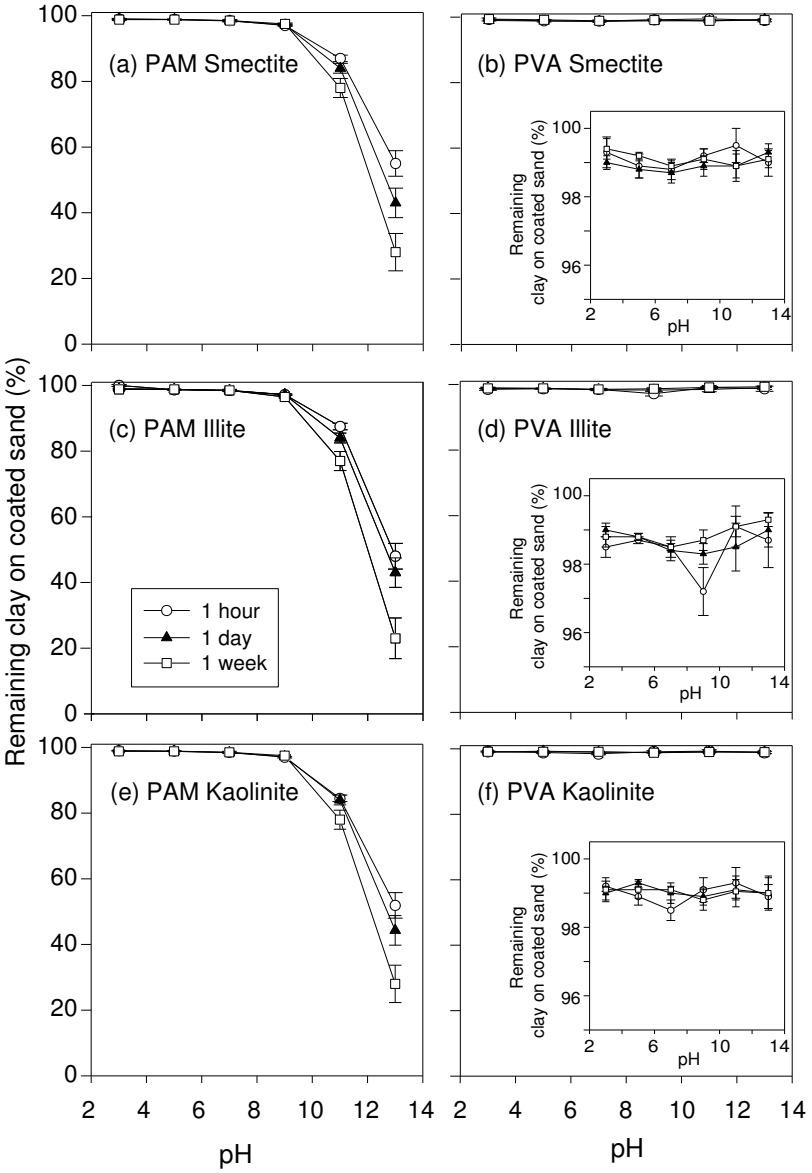

Figure 2.8: pH stability of coated clays of (a,b) smectite-coated sand, (c,d) illite-coated sand, and (e,f) kaolinite-coated sand. The left column (a,c,e) shows results of sand coated with the polyacrylamide (PAM) method, and the right column (b,d,f) shows results of sand coated with the polyvinyl alcohol (PVA) method. Inserts show a magnification of the PVA panels. Error bars denote one standard deviation of three repetitions.

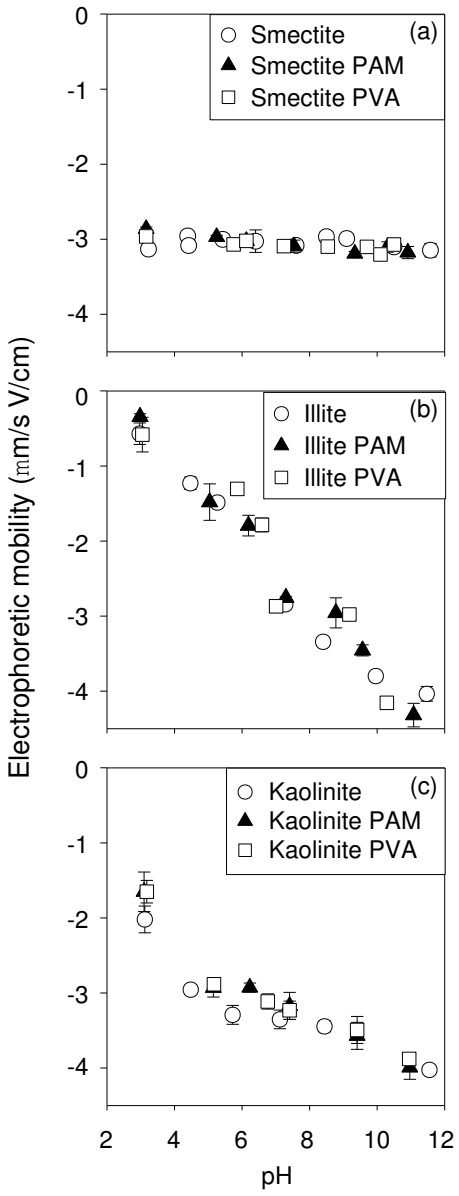

Figure 2.9: Electrophoretic mobility of pure clay and clay-polymer complex: (a) smectite (STx1), (b) illite (No. 36, Morris), and (c) kaolinite (KGa1). Error bars denote one standard deviation.

2.7 Appendix A

2.7.1 Preparation of Clay Minerals

Clean clay by removing iron, carbonates, and organic matter. Sieve and fractionate the clays to obtain particles less than 2 μm in diameter.

2.7.2 PAM clay coating procedure

Preliminary steps

- Prepare a clay suspension of 4 g/L, adjusted to pH 7 with 0.1 M NaOH.
- Get clean sand (immerse in 2 M HCl at 80 °C over night)
- Prepare PAM solution at concentration of 100 mg/L.

Coating Procedure

1. Sonicate clay suspension for 10 minutes.
2. Take 100 mL of clay suspension (4 g/L) and add 100 ml of PAM (100 mg/L) at room temperature in a 500 mL polypropylene tube. This yields a clay mass of 400 mg and a final polymer concentration of 50 mg/L. (Note: Do not use a PAM stock solution as high as in case of PVA.)
3. Let the clay polymer complex settle down for a couple hours (2-3 hours) at room temperature, collect the slurry, and discard the supernatant.

4. Gently mix the slurry with the sand (80 g of sand; clay-to-sand ratio = 1:20) with a plastic spatula.

5. Put on a reciprocal shaker over night. Shake at about 120 rpm.

6. Put the sand in the oven at 100 °C and dry for 24 hours.

7. After drying, wash loose particles with deionized water several times and dry again at 100 °C for 24 hours.

2.7.3 PVA clay coating procedure

Preliminary steps

- Prepare a clay suspension of 40 g/L adjusted to pH 5 with 0.1 M HCl.
- Shake on reciprocal shaker the suspension overnight.
- Get clean sand (immerse in 2 M HCl at 80 °C over night).
- Prepare PVA solution at a concentration of 1 g/L by dissolving PVA in warm water.

Coating Procedure

To get the mass of clay needed, you need to determine the amount of clay that you want to load over the sand surface. Usually, around 50% of the clay is loaded on the sand surface.

1. Sonicate clay suspension for 10 min.

2. Mix 25 mL of clay suspension (=1000 mg clay) with 2 mL of PVA solution (=2 mg PVA) at room temperature in a 100 mL centrifugal tube.

3. Shake the mixture for 10 minutes on a reciprocal shaker.

4. Then add the clay-PVA mixture to sand (10 g of sand to obtain clay-to-sand ratio = 1:10 w/w) in a beaker.

5. Put in oven at 50 °C, until the water is completely evaporated (the solution surface is 1-2mm above the sand surface). (Note: To obtain a more uniform coverage use the lower temperature. The temperature could go up to 80 °C, but at high temperature is difficult to control the coverage of the clay on the sand surface.)

6. Gently mix the clay-sand suspension every 10 to 15 minutes with a plastic stirrer by hand. Pay attention especially at the moment when all the water is evaporated, and mix very thoroughly. This step helps to get a more uniform coverage.

7. After all the water is evaporated, but before the sand is completely dry (There is a stage after the water is evaporated and the sand looks dry, at this moment the sand grain separate easily and does not glue back together, separation at this stage allows to obtain the most uniform coverage and the lowest amount of clay particles lost), take out the clay-coated sand and separate the sand gently

with a mortar and pestle. (Note: If this step is not done, the sand becomes a large agglomerate. To separate it, it will be necessary to break it apart and a large amount of clay is lost.)

8. Place the clay-coated sand back into oven over night at a temperature of 80 °C.

9. Take out the clay-coated sand and cool to room temperature.

10. Sieve the clay-coated sand through a 500 μm sieve to remove the sand coated by excessive clay.

11. After this, clean the sand by washing/gently rinsing with deionized water to remove all loose particles, and dry at 80 °C for 24 hours.

Chapter 3

Humic Acid, Ferrihydrite, and Aluminosilicate Coated Sands for Column Transport Experiments

3.1 Abstract

Interactions of chemicals with soil minerals are often studied in batch systems. Dynamic flow systems are often limited by the low hydraulic permeability of the soil constituents, such as clays, when packed into columns. However, immobilization of clay minerals and organic matter on an inert support allow perform experiments in dynamic flow systems. In this study, we investigate the feasibility to produce porous media with similar hydrodynamic properties, but different surface characteristics. Four minerals (ferrihydrite, kaolinite, illite, and smectite) and a humic acid were coated on silica sand grains. Coated grains were packed into columns and the hydrodynamic

This chapter has been submitted for publication: Jerez, J., and M. Flury, Humic Acid, Ferrihydrite, and Aluminosilicate Coated Sands for Column Transport Experiments.

properties of the media were determined with conservative tracers. The hydrodynamic properties of the various coated silica sands were similar, suggesting that porous media with similar spatial structure, but different surface characteristics, could be produced. Coating of clay minerals was shown to cause anion exclusion of anionic tracers when high surface charge clays or high clay loadings for the coating procedure were used. The specific surface area of the coating materials inside the porous medium could be changed by varying the particle size of the silica grain support. Coating of different materials onto silica sand grains allows to study interactions of chemicals and colloids with dynamic flow experiments in a porous medium with defined structure.

3.2 Introduction

Clays, organic matter, and iron- and aluminum-oxides, are the most reactive solid constituents in soils and sediments. These materials play a major role in the fate and transport of contaminants. Studies with pure minerals have provided mechanistic insight about solid-liquid phase interactions of a variety of chemicals with mineral surfaces [*Stumm,* 1992]. Batch sorption experiments are a standard protocol to study interactions of chemicals with soils and sediments, and to derive sorption coefficients and equilibrium constants. An alternative approach to derive the latter parameters are column transport experiments. Column transport experiments have certain advantages over batch sorption studies, i.e., the experimental conditions may be more representative of natural conditions in a flow-through column than in a batch reactor.

However, many solid materials are not suitable for column experiments, because of their small particle size which may cause columns to clog up [*Wibulswas,* 2004]. Coating of such materials on an inert support, such as sand or glass beads, would allow performing column transport experiments with a structurally stable and hydraulically conductive porous medium. Indeed, iron-oxides have been successfully coated on silica sand particles [*Scheidegger et al.,* 1993*; Schwertmann and Cornell,* 2000] and used for studying humic acid interactions with iron-oxides [*Gu et al.,* 1996b] and the transport of heavy metals [*Benjamin et al.,* 1996] and radionuclides [*Hansen et al.,* 2001]. Humic acid has been coated on silica beads to obtain porous materials suitable for chromatographic separations (e.g., *Szabo et al.,* 1995*; Yang and Koopal,* 1999*; Laor et al.,* 2002). It has recently been shown that clay minerals can be coated on silica sand and glass beads [*Ake et al.,* 2001].

This possibility to coat silica sands or glass beads with iron-oxides, humic material, and clay minerals offers the opportunity to study the interactions of solutes with three major soil constituents using dynamic column experiments. If the soil constituents are coated on the same silica sand or glass bead matrix, then we can construct porous media which have similar structure, but have different surface characteristics.

The objective of this work was to investigate the hydrodynamic properties of porous materials (packed silica sand) coated with different soil constituents. We hypothesized that we can construct porous media with similar hydrodynamic properties, but different surface characteristics. Furthermore, we tested whether we can modify the

hydraulic properties without changing the surface characteristics of the medium. Our experimental approach was to coat silica sand with humic acid, ferrihydrite, or clay minerals, and to compare the transport of tracers through columns packed with coated sand material.

3.3 Materials and Methods

3.3.1 Silica Sand and Sand Pretreatment

Silica sand (J.T. Baker, Phillipsburg, NJ; CAS No. 14808-60-7) was fractionated by dry sieving to obtain particles between 0.25 mm and 1 mm diameter. The sand was treated with H_2O_2 to remove organic matter [*Kunze and Dixon,* 1986] and with citrate-dithionite to remove iron [*Holmgren,* 1967]. Then the sand was extensively rinsed with deionized water and oven dried at 110°C.

3.3.2 Humic Acid Coating of Silica Sand

Humic acid was obtained from Aldrich (Lot No. 03130JS). We coated the humic acid over the silica sand following the methodology developed by *Koopal et al.* [1998]. This procedure involved modification of the silica surface with 3-aminopropyl-triethoxysilane (APTS) (Aldrich, MI) [*Vrancken et al.,* 1995*; Koopal et al.,* 1998*; Yang and Koopal,* 1999]. The amount of humic acid coated on the sand was determined by detachment of the humic acid in 1 M NaOH followed by quantification with UV/VIS spectrometry

(HP 8452A, Hewlett Packard) at a wavelength of 254 nm. The spectroscopic measurements were calibrated with a TOC analyzer (TOC 5000, Shimadzu Corporation, Kyoto, Japan).

3.3.3 Ferrihydrite Coating of Silica Sand

Ferrihydrite (6-line ferrihydrite) was synthesized according to *Schwertmann and Cornell* [2000, *p. 104–105*]. For the synthesis, Pyrex glass beakers were used. After synthesis, the ferrihydrite was dialyzed at room temperature (20–22°C) until the electrical conductivity of the solution was less than 5 μS/m.

We coated the silica sand with ferrihydrite using a slightly modified procedure developed by *Scheidegger et al.* [1993]. We carried out initial experiments to test optimal concentration and pH at which a homogeneous and extensive coating of silica sand with ferrihydrite was obtained. Briefly, 40 mL dialyzed ferrihydrite suspension was mixed with 60 g silica sand, and shaken for a total of three days. The pH of the initial solution was 6.5, and after one day of shaking, the pH was adjusted to 7.0 with 0.01 M NaOH, and after another day to pH 7.5. Finally, the sand was washed three times with 1 M HNO_3 and 10 M NaOH. The amount of Fe coated over the sand was determined by dissolution of ferrihydrite with 2 M HCl at 80°C for 12 h, followed by quantification of Fe by Atomic Absorption Spectroscopy (Varian 220 Flame Atomic Absorption Spectrometer). The mineralogical stability of ferrihydrite was verified with X-ray diffraction (Philips XRG 3100, Philips Analytical Inc., Mahwah NJ).

3.3.4 Aluminosilicate Coating of Silica Sand

Four clay minerals, Georgia kaolinite (KGa1), Arizona smectite (SAz1), Texas smectite (STx1) (Clay Minerals Repository, University of Missouri), and illite (No 36, Morris, Illinois, Ward's Natural Science, Rochester, NY), were selected to be coated over the sand. The clay minerals were treated to remove organic matter using H_2O_2 [*Kunze and Dixon,* 1986] and iron oxides using citrate-dithionite [*Holmgren,* 1967], and were then fractionated to obtain particles < 2 μm in hydrodynamic diameter using gravity sedimentation. The clay minerals were made homoionic by washing with 1 M NaCl (KGa1), 0.5 M $CaCl_2$ (SAz1 and STx1) or 1 M KCl (Illite) [*van Olphen,* 1977]. Finally, the clays were dialyzed with deionized water until the electrical conductivity of the solution was less than 5 μS/m.

The clay minerals were coated over the sand surface using the procedures described in the chapter 2 of this dissertation. Briefly, clay suspensions were flocculated with 50 mg/L polyacrylamide (Superfloc C498, Cytec Industries, West Paterson, NJ). The mixture was left to settle down, and then centrifuged at 100 g for five minutes. Then, the clay-polymer complex slurry was mixed with the silica sand and dried at 100°C for 24 h. The coated sand was then washed with deionized water and dried again at 100°C for 24 h. The amount of clay coated over the silica sand was determined by detaching the clays with 1 M NaOH. The amount of detached clay minerals were quantified by UV/VIS spectrometry at a wavelength of 230 nm.

We chose the different clay minerals to represent major types of aluminosilicate

clays. The two smectites differed with respect to surface charge. The cation exchange capacity (CEC) of SAz1 (123±3 $mmol_c$/100 g) is around 40% greater than that of STx1 (89±2 $mmol_c$/100 g) [*Borden and Giese,* 2001]. This allowed us to assess the effect of surface charge on transport of anionic tracers.

3.3.5 Surface Characterization of Soil Constituents and Coated Sands

Specific surface areas were determined with N_2 adsorption (ASAP2010, Micromeritics, Norcross, GA) based on BET isotherms. We measured the surface areas of the minerals and humic acid before coating onto the sands, and then measured the surface areas of the coated sands. The isoelectric point (IEP) for ferrihydrite and kaolinite was measured in a 1 mM NaCl background with dynamic light scattering (Zetasizer 3000 HSA, Malvern Instruments Ltd., Malvern, UK). The IEP of Aldrich humic acid was taken from *Koopal et al.* [1998]. For kaolinite, ferrihydrite, and humic acid coated sands, the point of zero salt effect (PZSE) was measured by the salt addition method [*Benjamin et al.,* 1996]. About 20 g of the coated material was packed into a column, and 20 mL of 0.01 M $NaNO_3$ was recirculated at a rate of four pore volumes per minute. The pH was monitored with a flow-cell electrode. When the pH was equilibrated, 0.4 mL of 5 M $NaNO_3$ was added to increase the salt concentration by a factor of 10, and the pH change was monitored. This was done with initial pH values ranging from 2 and 9. The PZSE was obtained when no pH change was observed after the

addition of the high concentration salt solution. Although the IEP and the PZSE are different and cannot be compared [*Sposito,* 1998], they gave some indication about the overall surface charge characteristics of the particles. The surface morphology of the coated sands was examined by scanning electron microscopy (Hitachi S520, Hitachi Instruments, Inc., Tokyo, Japan).

3.3.6 Column Transport Experiments

Column experiments were performed in a borosilicate glass column of 1.5-cm diameter and 12-cm length (Omnifit, Cambridge, UK). The column end pieces were of Teflon with frits of 40 μm pore diameter. The column was packed with clean or coated sands under saturated condition. The solution background consisted of an electrolyte mixture with 4.45 mM $CaCl_2$, 1.4 mM $MgCl_2$, 0.4 mM KCl, 0.7 mM and NaCl, with an ionic strength of 18.55 mM. This solution mimics soil pore water. The background solution was pumped through the column from the bottom using a peristaltic pump (Ismatec, Switzerland). At least 20 pore volumes were flushed through the column to equilibrate the system before the tracer experiment.

Column breakthrough curves were determined using nitrate (0.2 mM $NaNO_3$) or bromide (0.2 mM KBr) as tracers spiked to the background electrolyte solution. The tracer concentration was measured online with a flow cell and a diode array spectrophotometer; NO_3^- was measured at a wavelength of 220 nm and Br^- at 202 nm. Calibrations of tracer standards followed Beer's law. Tracers were fed into the column

as pulses of two to four pore volumes.

Column breakthrough curves were analyzed to determine the pore water velocity v and the hydrodynamic dispersion coefficient D using the advection-dispersion equation (ADE) and the code CXTFIT 2.1 [*Toride et al.,* 1995]. The Peclet number, Pe, was then calculated as $\mathrm{Pe} = vL/D$, where L is the length of the column.

Three different types of experiments were conducted. In the first set of experiments, we evaluated the hydrodynamic dispersion of the coated sands (humic acid, ferrihydrite, kaolinite, illite and Texas Ca-smectite-coated silica sands). A constant flow rate of 1.2 mL/min was used for these experiments. The second set of of experiments was used to evaluate the effect of grain size of the coated sands on the hydrodynamic properties of the porous materials. For these experiments, we fractionated the Texas smectite coated sand by sieving into two fractions, with particle diameters from 255 to 355 μm and 425 to 500 μm, respectively. The third set of of experiments was used to investigate the behavior of an anionic tracer in ferrihydrite-coated sand, and two types of high-load smectite-coated sands. The high-load coated sands were obtained by using the polyvinyl alcohol methodology described in chapter 2. Each breakthrough curve was repeated at least twice. Replicates were reproducible, and we therefore only show one breakthrough curve for each experiment.

3.4 Results and Discussion

3.4.1 Surface Characterization of Coated Sands

Figure 4.3 shows images of coated silica sand surfaces. The clean silica surface depicts an irregular topography (Figure 4.3A). The coatings covered the silica surface incompletely, there were always some portions of the surface that were not covered by coatings. Based on screening of the images, we estimate that about 80% of the surface was covered by coatings. Incomplete surface coating of iron-oxides was also observed by others [*Scheidegger et al.*, 1993].

Quantitative characteristics of the coated sands are listed in Table 3.1. The amount of humic material and minerals that could be coated onto the silica grains was in the range of 1 to 25 mg per gram of sand, except for the clay coating with the polyvinyl alcohol method, which resulted in higher surface coverage. The coated sands had a PZSE similar to that of the coating materials. The specific surface areas of the coated sands were about two orders of magnitude smaller than the surface areas of the coating materials itself, but considerably larger than that of the uncoated sand. The amount of coating per surface area was calculated from the measured specific surface area and the amount of coating per mass.

The amount of humic acid that we could coat onto the sand was around 1 mg per gram of sand (Table 3.1), which is similar to the result obtained by *Laor et al.* [2002] using sol-gel immobilization. *Koopal et al.* [1998] reported a surface coverage

of humic acid of 63 mg/g, but used a much smaller silica support (silica beads of 40 nm diameter) than we did. On a per surface area basis, our 26 mg/m^2 compares with 1.2 mg/m^2 from *Koopal et al.* [1998]. The higher surface loading obtained in our experiments is likely due to multilayer coverage (Figure 4.3B), compared to monolayer coverage in *Koopal et al.* [1998].

The amount of ferrihydrite coating was 4.4 mg Fe/g, which is in the range reported by *Scheidegger et al.* [1993]. The IEP for the ferrihydrite mineral was pH 6.8, which is low for iron oxides but can be explained by inclusion of small amounts of silica [*Anderson and Benjamin,* 1985]. The surface area of the coated sand was one order magnitude larger than that of the clean sand, in agreement with published data [*Benjamin et al.,* 1996]. The specific surface area of ferrihydrite (65 m^2/g) was smaller than that reported by *Nègre et al.* [2004] (301 m^2/g). We attribute this difference to possible aggregation of our ferrihydrite during freeze-drying. X-ray diffraction measurements confirmed the presence and stability of 6-line ferrihydrite before and after coating.

Aluminosilicate clays coated on silica sand using the polyacrylamide method had similar specific surface areas as the iron-oxide-coated sand (Table 3.1). A one order magnitude larger surface area was obtained for sand coated with polyvinyl alcohol. For the aluminosilicate clays, the IEP was only determined for kaolinite, but not for illite and smectite which have a permanent structural negative charge. The IEP for kaolinite minerals was pH 2.4, and the PZSE of kaolinite-coated sand was pH 2.9.

3.4.2 Column Transport Experiments

Figure 3.2 shows breakthrough curves of conservative tracers in coated sand media. Nitrate did not behave as conservative tracer in ferrihydrite-coated sand. We used Br^- as tracer, which behaved conservatively at pH 9.9. The breakthrough curves could be well described by the ADE for a conservative chemical, and the model parameters are listed in Table 3.2. Measured and estimated pore water velocities were very similar. The different coated sands had similar hydrodynamic dispersion coefficients and Peclet numbers, indicating that all porous media possessed similar hydrodynamic properties. This suggests that we can generate porous media with similar hydraulic properties, but different surface characteristics.

We used two anionic tracers, Br^- and $NO_3{}^-$, to assess the hydrodynamic behavior of the coated sands. For ferrihydrite-coated sands, we expected both Br^- and $NO_3{}^-$ to be a conservative tracer when the solution pH was well above the IEP of ferrihydrite. A series of breakthrough curves conducted at different pH values showed that $NO_3{}^-$ was retarded at pH 4.1, and as the pH was raised, the retardation became less and less (Figure 3.3). However, even at pH$\approx$10, several pH units above the IEP of ferrihydrite, $NO_3{}^-$ was retarded as compared to Br^-, which behaved conservatively (Figure 3.3). At pH 7.4 we also observed retardation of Br^-, as would be expected because the ferrihydrite picks up more positive charges (data not shown). The observation that Br^- moved faster than $NO_3{}^-$ may be attributed to different sorption characteristics of the two ions [*Sposito,* 1989*; Clay et al.,* 2004].

Anionic tracers may be subject to anion exclusion during transport in a porous medium that has highly negative surface charges [*Sposito,* 1989]. Anion exclusion results in an early breakthrough of the anionic tracer, and has been observed repeatedly [*Bowman,* 1984*; James and Rubin,* 1986*; Schoen et al.,* 1999]. The higher the negative surface charge of the minerals, the more anion exclusion would be expected. We can readily demonstrate these effects using different clay loadings and differently charged clays (Table 3.1). Silica sand coated with a small amount of smectite (STx1 low load) showed no anion exclusion, indicated by the superposition of its NO_3^- breakthrough with the one obtained in clean silica sand (Figure 3.4). On the contrary, anion exclusion was observed for the high-load smectite-coated sand (STx1 high load) as well as for the SAz1-smectite-coated sand. Such anion exclusion effects may need to be considered when using these latter types of coatings.

The NO_3^- breakthrough curves for STx1 and SAz1 smectites were very similar. The SAz1 smectite has a 40% higher CEC than the STx1 smectite [*Borden and Giese,* 2001], from which we would expect more anion exclusion in the SAz1-coated sand. However, the specific surface area of the SAz1-coated sand was about 50% less than that of the STx1-coated sand. Consequently, the overall anion exclusion effect in these two porous media was similar.

Changing the grain size of the silica support allowed manipulation of the specific surface area of the coated porous medium as well as the amount of coating per unit mass of the porous medium. As an example, we show the coating of smectite (STx1)

on silica grains with two different diameter ranges (Table 3.3). The specific surface area of the coated sand was doubled when the grain size of the support silica was reduced from 425–500 to 250–355 μm. A corresponding increase in the amount of clay coating per unit mass of porous medium was observed as well. The amount of clay coated per surface area of sand was similar, supporting that the increase in specific surface area was due to the decrease in grain size. Figure 3.5 illustrates that changing the grain size does not necessarily affect the hydrodynamic dispersion of the porous medium. The breakthrough curves of NO_3^- were similar among the two clay-coated porous media, the uncoated sand, and also among the coated sands of different grain diameters. While the hydrodynamic dispersion did not change, the hydraulic conductivity obviously changed as the grain size changed.

3.5 Conclusions

Ferrihydrite-, aluminosilicate clay-, and humic acid-coated sand grains can be packed into columns and be used to study interactions of chemicals or colloids with the coating materials under dynamic flow conditions. Coated sand packings had the same hydrodynamic properties (Peclet numbers) as the uncoated sand packing. The coating of the silica grains allows to generate a permeable and structurally stable hydrodynamic system, yet with surface properties of colloidal-sized particles. Clay-coated silica sand media can cause anion exclusion, depending on the amount of clay coated onto the silica surfaces and the surface charge of the clays used. Such anion exclusion can be

determined using a tracer breakthrough experiment. The specific surface area of the coating materials on the silica grain support can be manipulated by selecting different particle sizes of the silica grains. The hydraulic conductivity of the system can be readily adjusted by selecting an appropriate particle size of the silica support grains.

3.6 Tables and Figures

Table 3.1: Characteristics of humic acid, minerals, and coated sands.

Material	Specific Surface Area	IEP/PZSE[a]	Amount of Coating	
	(m^2/g)	(pH)	(mg/g)	(mg/m^2)
Coating Materials				
Humic Acid (Aldrich)	5.9±0.3[b]	2.8[c]	none	none
Ferrihydrite	65.3±0.8	6.8	none	none
Kaolinite (KGa1)	13.6±0.3	2.4	none	none
Illite (No. 36, Morris)	36.5±0.4	none	none	none
Texas smectite (STx1)	52.6±0.5	none	none	none
Arizona smectite (SAz1)	25.1±0.9	none	none	none
Sands				
Control, uncoated sand	0.04±0.001	3.2	none	none
Humic Acid coated sand	0.21±0.01	3.4	1.04 ± 0.03	26
Ferrihydrite coated Sand	0.4±0.01	6.7	4.4 ± 0.2	109
Kaolinite coated sand	0.24±0.01	2.9	24.7± 3.2	618
Illite coated sand	0.29±0.01	none	5.0± 0.4	126
Smectite-(STx1)-coated sand (low load)	0.35±0.01	none	3.1± 0.2	77
Smectite-(STx1)-coated sand (high load)[d]	2.41±0.02	none	32.3± 3.5	808
Smectite-(SAz1)-coated sand (high load)[d]	1.20±0.01	none	54.1± 5.1	1354

[a] IEP: isoelectric point of coating materials; PZSE: point of zero salt effect for sands.

[b] errors denote one standard deviation.

[c] from *Koopal et al.* [1998].

[d] clay coating using the polyvinyl alcohol methodology.

Table 3.2: Summary of experimental and modeled breakthrough curves.

	Measured		Fitted ADE parameters			
Treatments	Porosity	Pore water velocity	Pore water velocity	Hydrodynamic Dispersion	Peclet Number	R^2
	(%)	(cm/min)	(cm/min)	D (cm^2/min)	Pe	
Clean sand	35.1	1.97	1.95	0.25±0.01[a]	93±4	0.999
	coated sands					
Humic acid	33.2	2.07	2.07	0.27±0.03	91±9	0.999
Ferrihydrite	36.4	1.82	1.87	0.24±0.03	101±11	0.988
Kaolinite (KGa1)	34.2	1.87	1.89	0.23±0.01	99±4	0.989
Illite	37.5	2.04	2.07	0.23±0.02	102±8	0.998
Smectite (STx1)	38.2	1.89	1.88	0.22±0.02	104±9	0.999

[a] errors denote one standard deviation.

Table 3.3: Effect of sand size on clay coverage for smectite (STx1).

Silica Grains	Grain Diameter	Specific Surface Area	Clay Coverage	
	(μm)	(m^2/g)	(mg/g)	(mg/m^2)
Small grains	250–355	0.152±0.007	15.7±0.4	103.4±7.1
Large grains	425–500	0.086±0.004	10.9±1.3	126.9±21.1

The polyvinyl alcohol method was used for the coating.

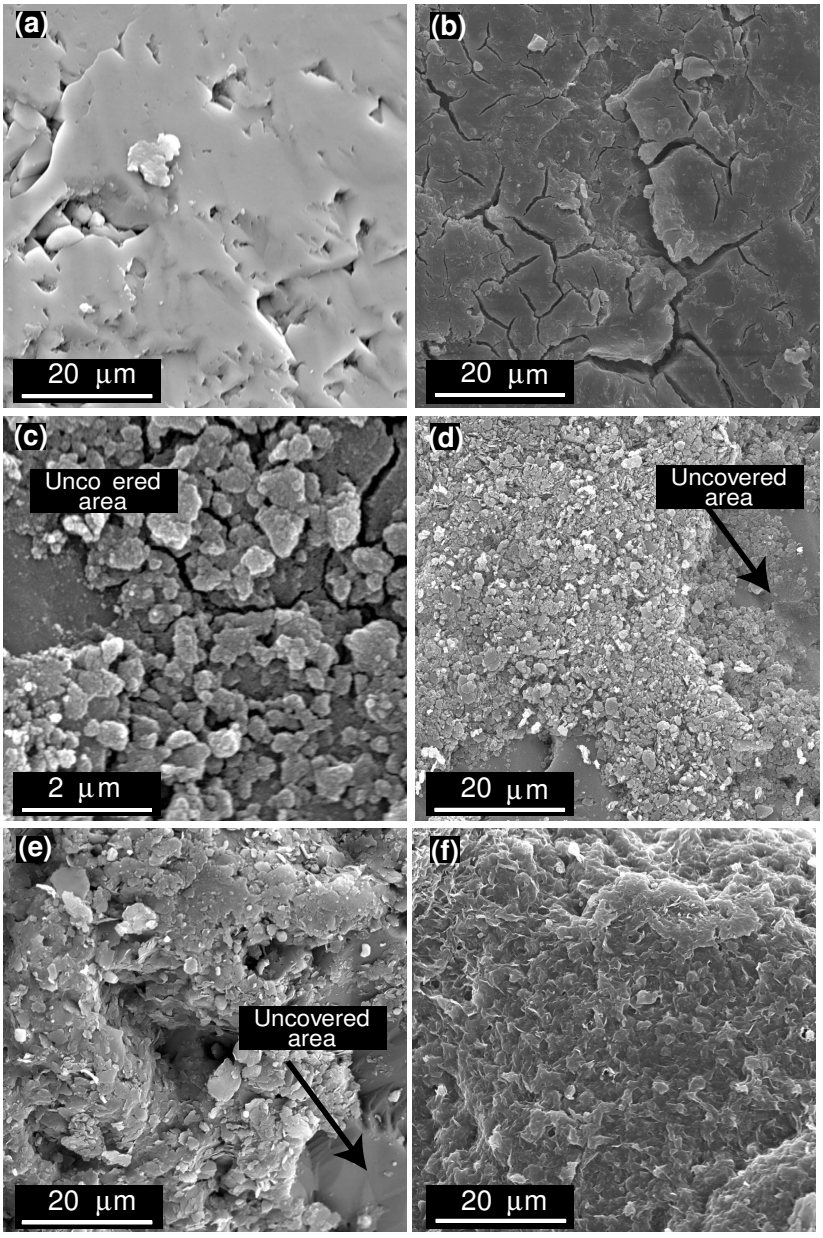

Figure 3.1: Scanning electron micrographs of (a) clean silica sand (control), (b) humic-acid-coated sand, (c) ferrihydrite-coated sand, (d) kaolinite-coated sand (KGa1), (e) illite-coated sand (No. 36, Morris), and (f) smectite-coated (STx1) sand. Note that the scale of the ferrihydrite micrograph is different than the other scales.

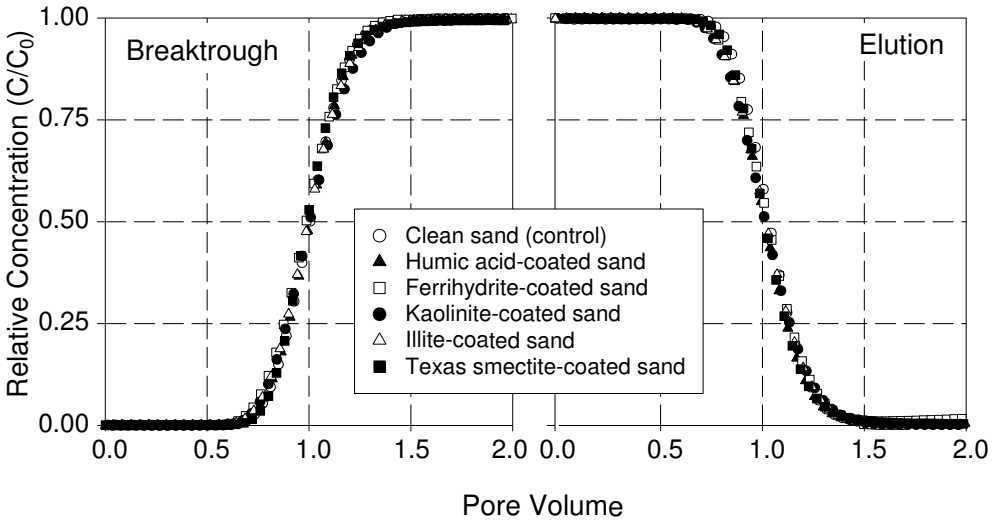

Figure 3.2: Breakthrough curves of conservative tracers for different coated sands. In all cases NO_3^- was used as tracer, except for ferrihydrite-coated sand, where Br^- was used. The pH of the solutions was 6.5 to 7, except for ferrihydrite-coated sand, where the pH was 9.9.

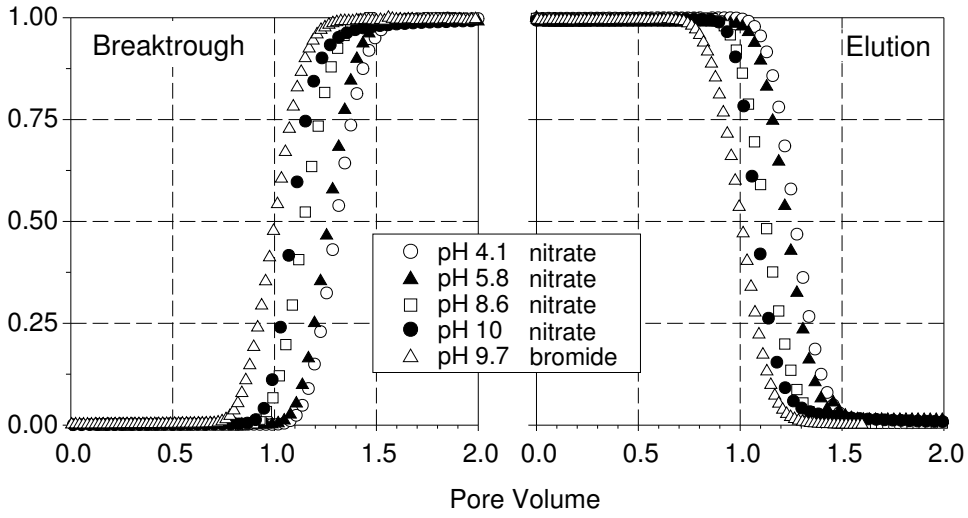

Figure 3.3: Effect of pH on NO_3^- breakthrough curves in ferrihydrite-coated sand. The breakthrough curve for Br^- at pH 9.7 is shown as an example of a conservative tracer.

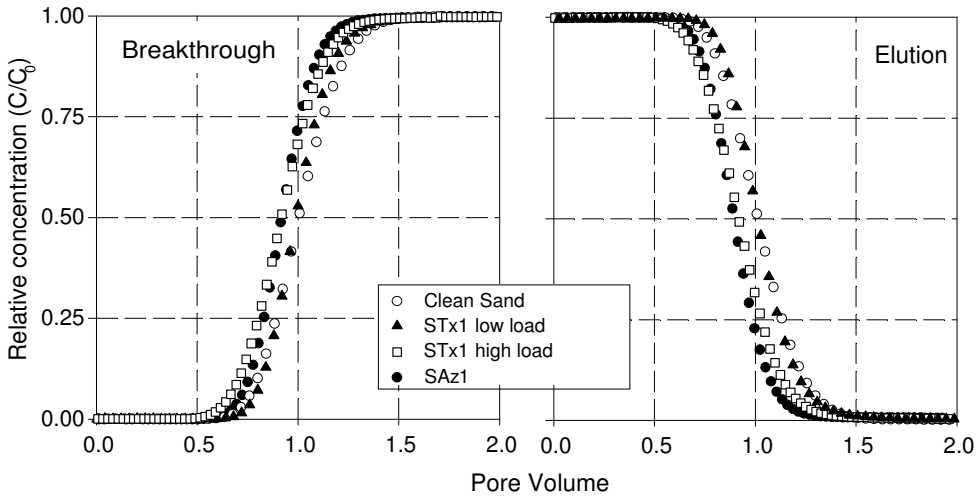

Figure 3.4: Effect of clay loading on breakthrough curves of NO_3^- in smectite-coated sand.

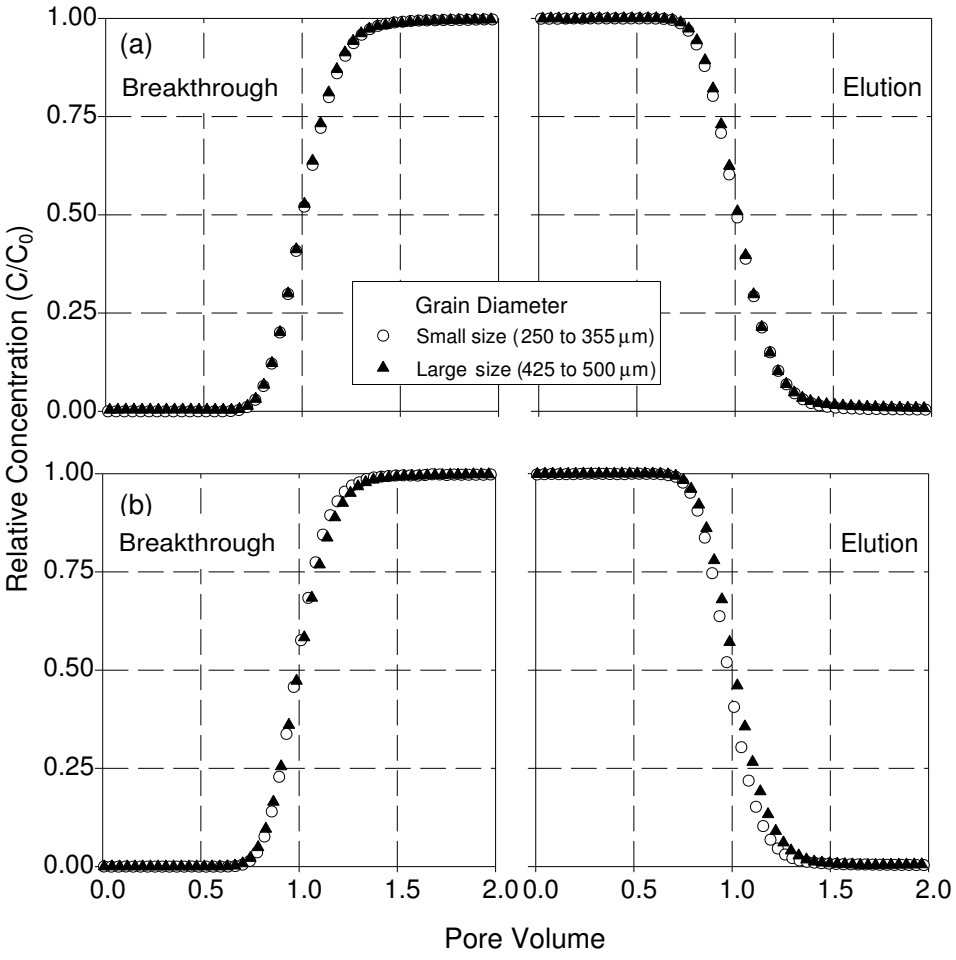

Figure 3.5: Effect of sand particle size on breakthrough curves of NO_3^-. (a) Uncoated silica sand and (b) STx1-smectite-coated sand.

Chapter 4

Interaction of Humic Acid with Clay Minerals in Dynamic Flow Systems

4.1 Abstract

Humic acids play an important role in the movement and fate of heavy metals and organic molecules. Transport of humic acids in a porous medium have been identified as a potential carrier for contaminants. The study of the interaction of humic acids and clay has been restricted to batch experiments and no dynamic flow studies with humic acids in clay-sand porous media have been conducted. The objective of this study was to investigate the transport of a commercial humic acid through a porous medium dominated by clay minerals. We conducted column experiments with porous media dominated by kaolinite, smectite, and illite immobilized on the surface of silica sand through a polyvinyl alcohol coating method. Humic acids were injected into the columns at pH 7.5 and a concentration of 10 mg/L of organic carbon. The clay-coated sand sorbed a large amount of humic acid. The relative concentration of humic acid

in the column outflow was always lower than 0.4 in all the clay-coated sand. A significant amount of humic acids moved quickly through the porous media, especially in the kaolinite-coated sand. Repeated injection of humic acid resulted in a steeping of successive breakthrough curves than imply limiting sorption sites on the sand surfaces. This research showed that a significant fraction of the humic acid moved quickly through the porous media dominated by clay minerals. A model with the Freundlich isotherm and irreversible sorption parameter was the best model to fit the observed data.

4.2 Introduction

The term "humic acid" stands for a large collection of organic molecules of non well-defined structures and large range of molecular size. Humic acids are ubiquitous in terrestrial and aquatic environments. These molecules play important roles in the transport and fate of organic molecules and heavy metals [*Chiou et al.*, 1986; *Tipping*, 2002; *MacCarthy*, 2001].

Humic acids have the capacity to sorb large amounts of natural and anthropogenic organic molecules such as pesticide and hormones, as well as heavy metals and radionuclides [*Tipping*, 2002]. The sorption mechanism reduces the pollutant movement and helps to prevent groundwater contamination [*Guo et al.*, 1993]. However, *Graber et al.* [1995] studying the use of municipal wastewater, found that the organic molecules present in the wastewater enhanced the transport of atrazine, showing that the inter-

action between the humic material, the soil matrix, and the solutes are highly complex.

The potential of humic acids to facilitate the movement of contaminant in a natural environment will depend on the transport properties of the humic acids. Miscible transport experiments using iron-coated sand have shown that there is preferential sorption for large molecules with higher aromaticity [*Gu et al.,* 1996a*; Gu et al.,* 1996b*; McCarthy,* 2001*; Hur and Schlautman,* 2003*; Chorover and Amistadi,* 2001]. Similar results were reported from batch experiments using kaolinite and humic acids [*Balcke et al.,* 2002]. Humic acids of higher molecular weight and lower surface charge present higher affinity for the kaolinite surface [*Balcke et al.,* 2002*; Chorover and Amistadi,* 2001]. Both kaolinite and humic material present negative surface charges at pH larger than 3 ([*Koopal et al.,* 1998], and see chapter 3), therefore humic acids with less surface charge have less repulsive forces. High molecular weight humic acids have less polar groups and tend to be more hydrophobic than low molecular weight humic acids [*Shin et al.,* 1999]. However, it was also demonstrated that after the binding sites were filled, humic material could move in similar patterns as a conservative tracer [*Dunnivant et al.,* 1992].

In contrast to kaolinite, montmorillonite clay has a tendency toward preferentially sorb low-molecular weight humic material compared to high-molecular weight molecules, but seems to have no preferential sorption of aromatic compared to the aliphatic functional group [*Chorover and Amistadi,* 2001]. Infrared data showed that the binding mechanism involved was water or cation bridging. The authors also found

that the amount of humic acid sorbed by the montmorillonite was higher than in the case of kaolinite, mainly due to the larger surface area of the montmorillonite clay [*Chorover and Amistadi,* 2001].

Little information is available on humic acid transport through clay-dominated porous media, mainly because column experiments with clays are inconducent due the low hydraulic conductivity. In this research we studied the transport properties of commercial humic acid on porous media dominated by different clay minerals. We used porous media dominated by the following clay minerals: Georgia kaolinite, Morris illite and Texas smectite.

4.3 Review of Humic Acids

4.3.1 Origin, Chemical Structure and Properties

Humic material is a large and heterogeneous group of macromolecules of different molecular weight and charge density [*Stevenson,* 1994], with complex and difficult identifiable structure [*Senesi,* 1993*; Gaffney et al.,* 1996b*; De Paolis and Kukkonen,* 1997]. There is no evidence of biological or genetic control in the origin of humic materials nor of biological function [*Haynes,* 1991], therefore they do not meet any structural criteria applied to other macromolecules like proteins. The main chemical groups present in humic materials are aromatic and aliphatic groups, and small amounts of amino acids, amino sugars, and fatty acids [*Stott and Martin,* 1990]. Although, hu-

mic materials are the result of the decomposition of plant and animal tissues, there is little resemblance between the parent material and the humic acids [*Haynes,* 1991]. The processes by which humic substances are generated have been studied for a long time but are still not well known. There are four major theories about the origin and synthesis of these molecules:

- The lignin theory: This theory, proposed by Waksman in 1932, states that the degradation products of the lignin will become a source of the aromatic structure of humic substances [*Wershaw,* 1986*; Oades,* 1989*; MacCarthy et al.,* 1990b*; Senesi and Loffredo,* 2001]. Aromatic compounds present in plants like lignin are more resistant to degradation, and contrary to protein and sugars, only 30% will decompose in a period of one year [*Stott and Martin,* 1990]. A modification of this theory proposed by Hatchey and Spiken in 1978 postulates that other biopolymers such as cutin and suberin are also precursors of the humic substances [*Senesi and Loffredo,* 2001].

- Microbial synthesis of aromatic: Other sources for aromatic group present in humic acid could be provided by fungi or microorganisms that produce melanin, which has properties similar to humus materials [*Stott and Martin,* 1990].

- The Maillard reaction theory: This theory states that the reaction between reduced sugar and amino substances (amino acids, peptides and proteins) produces a polymeric substance which appears to have properties like humic acids and could be one of the paths to produce humic acids [*Stott and Martin,* 1990].

- Quinone-amino acid interaction: This theory states that the lignin is completely degraded to aromatic compounds that are transformed to quinones. The quinones become polymers and react with amino compounds that form the humic materials [*Oades,* 1989*; Wershaw,* 1994].

Nevertheless, there is no consensus that these theories explain the origins of the humic materials [*Steelink,* 1999], probably because humic materials have multiple origins and large numbers of pathways lead to their formation [*Stevenson,* 1994*; Haynes,* 1991].

As of today there is no defined structure of humic materials or of basic units by which humic substances are built, some theoretical models have been developed which enable the prediction of its behavior in natural environments. There are two opinions about the nature of the humic substance structure. Some researchers consider that humic substances are true macromolecules with molecular weights as high as 300,000 KDa [*Swift,* 1999]. However, other researchers have questioned this concept and proposed that humic acids are micelle-like aggregates, with molecular weights no larger than 20 KDa [*Wershaw,* 1986*; Wershaw,* 1994*; von Wandruszka,* 1998*; Wershaw,* 1999]. In this model molecules have oriented hydrophobic moieties to the interior and a hydrophilic exterior surface; hydrophobic molecules found a "friendly" environment in the interior of the micelle [*Shulten,* 1996*; von Wandruszka et al.,* 1999]. At low pH and high concentration, humic acid has a random coil structure and at higher pH a linear and flexible chain [*Beckett et al.,* 1987]

Humic acids and fulvic acids are arbitrarily separated based on their solubility [*MacCarthy et al.*, 1990a; *Haynes*, 1991]. Humic acids contain more carbon and less oxygen than fulvic acids, and humic acids have larger molecular weight (10 K to 100 KDa) than fulvic acids (1 to 5 KDa).

4.3.2 Interactions of Humic Acid with Minerals

The humic acid-mineral interaction is pH dependent. Generally, the interaction is strongest at low pH but decreasing significantly at pH $>$ 5. In part, the enhanced interaction of humic acids at low pH is due to a decrease of negative charge, but also due to precipitation of macromolecules especially at very low pH. This behavior also shows that electrostatic interactions play an important role in the sorption of the humic material. Iron oxides, that have positive net surface charge up to pH 7.5 - 8.5 (isoelectric point (IEP) of iron oxides is between pH 7.5 and 8.5), present higher interaction with the humic acids. Aluminosilicate clays have lower IEP or permanently negative charge, therefore at higher pH, the electric repulsion between the humic acid and the aluminosilicate clay is enhanced. The IEP of the humic acid depends on the functional group present in the molecule. Carboxylic acid group is one of the most dominant in the molecules [*Stevenson*, 1994].

The mechanisms of interaction between humic acids and mineral surfaces are ligand exchange, cation bridging, entropy-driven and hydrophobic interaction [*Baham and Sposito*, 1994]. The ligand exchange mechanism has been proposed for the humic acid-

iron oxides interaction. Infrared data has shown that aluminosilicate clays interact with humic acid through water or cation bridging [*Chorover and Amistadi,* 2001].

Iron oxides sorbed more humic acid of high molecular weight than bulk humic acid molecules [*Gu et al.*, 1996a*; Gu et al.*, 1996b*; Chorover and Amistadi,* 2001*; McCarthy,* 2001*; Hur and Schlautman,* 2003]. The sorption process was hysteretic, due to the replacement of low-affinity molecules (low molecular weight and high charge density) with large humic molecules, showing that the "adsorption maxima" increased slowly over a long period of time [*Van de Weerd et al.,* 1999]. Similar behavior has been found with kaolinite, where humic acids of higher molecular weight and lower surface charge had higher affinity for the kaolinite surface [*Balcke et al.,* 2002*; Chorover and Amistadi,* 2001]. Both kaolinite and humic material present negative surface charge, therefore humic acids with less surface charge experience less repulsion. High molecular weight humic acids have less polar groups and tend to be more hydrophobic than low molecular weight humic acids [*Shin et al.,* 1999]. On the other hand, smectites clays have a tendency to preferentially sorb low molecular-weight humic material as compared to the large size molecules. However, research did not find preferential sorption of aromatic as compared to aliphatic functional groups [*Chorover and Amistadi,* 2001]. The amount of humic acid sorbed by smectites is higher than kaolinite. The main reason for this difference was the larger surface area of the smectite clays [*Baham and Sposito,* 1994*; Chorover and Amistadi,* 2001]

Transport experiments, using iron oxide coated sand and aquifer porous mate-

rial, have established that there is a pattern of preferential sorption of hydrophobic [*Dunnivant et al.,* 1992*; Gu et al.,* 1996a*; Gu et al.,* 1996b*; McCarthy*, 2001*; Hur and Schlautman,* 2003] and high-molecular weight fractions [*Gu et al.,* 1996a*; Gu et al.,* 1996b*; McCarthy*, 2001] as compared to the hydrophilic and low-molecular weight humic materials. In addition, a lysimeter study showed that small size humic acids could move similarly as a conservative tracer [*McCarthy*, 2001].

4.3.3 Organic Colloids Extraction, Fractionation, and Characterization

Humic materials are mixed with clays, minerals, polyvalent cations, and other non-humic organic materials. For that reason, extraction, fractionation, and characterization of this material is an important step that permits the study of homogeneous material. Several reviews have been published about the extraction and fractionation techniques [*Leenheer*, 1981*; Thurman and Malcolm,* 1981*; Aiken,* 1985*; Swift,* 1985*; Leenheer*, 1985*; Gaffney et al.,* 1996a*; Ambles*, 2001] and in the physical and chemical characterization of the humic materials [*MacCarthy et al.,* 1985*; Wershaw,* 1985*; Wershaw and Mikita,* 1987*; Bortiatynski et al.,* 1996*; Simpson et al.,* 1997*; Mao et al.,* 1998*; Xing et al.,* 1999*; Ambles,* 2001]. Different methods of extraction and fractionation have been developed to achieve different goals, but this has caused difficulties in the comparison of the results of different investigations. In addition, the chemical and physical characterization is not possible with only one technique; there-

fore the characterization of these materials is best made with several methods that permit obtaining different information of the sample. In this section these methods are reviewed with emphasis on the current methodology applied to the study of humic materials and their advantages and disadvantages.

Extraction Methods

Humic material is part of several other components of the organic matter of the soil. Its study requires that this material be separated from the inorganic matrix and non-humic organic matter [*Senesi and Loffredo*, 2001]. All of these methodologies use some extractant that must meet the following criteria [*Haynes*, 1985*; Swift*, 1996] :

- A high polarity and high dielectric constant to assist in the dispersion of the charge molecules.
- A small molecular size to penetrate into the humic structures.
- The ability to cut the existing hydrogen bonding and provide alternative groups to form humic-solvent hydrogen bonds.
- The ability to remove and immobilize metallic cations.

In addition *Stevenson* [1994] considers that the extraction methods must have the following objectives:

- The methods must avoid alteration of the materials isolated.

- The humic substances extracted must be free of inorganic contaminants like clays and polyvalent cations.
- Must be able to obtain complete extraction, which means that the methods should ensure representation of the entire molecular weight range.
- The methods should be applicable to all soils.

These criteria for extraction methods represent more ideal objectives than a set of achievable conditions [*Swift,* 1996].

One of the most used methods of extraction is the International Humic Substances Society (IHSS) methodology that is described in detail in *Swift* [1996]. One of the problems with this methodology is the use of hydrofluoric acids that change the structure of humic acids [*Swift,* 1996*; Senesi and Loffredo,* 2001]. Briefly, after the soil is sieved with a 2.0 mm sieve, the sample is mixed with 1 M HCl at a ratio of 1:10 (w/v) and shaken for 1 h at room temperature. Then the mixture is centrifuged at low speed and the supernatant is used to obtain fulvic acid. The soil residue is mixed with 1 M NaOH under N_2 atmosphere at ratio of 1:10 (w/v). This mixture is shaken for 4 h, and left overnight for settling. After that the mixture is centrifuged. The supernatant is separated and acidified with 6 M HCl under constant stirring to reprecipitate humic acids. After 12-16 h standing the suspension is centrifuged to separate the precipitated HA from the supernatant. The supernatant is passed through a XAD-8 resin to obtain fulvic acid [*Swift,* 1996]. An N_2 atmosphere is used to avoid the oxidation of phenols to semi-quinones and quinones functional groups of the humic acid [*Wershaw*

and Pinckney, 1977*; Engebretson and von Wandruszka,* 1997] that produce smaller size humic acid.

One of the goals of the extraction procedure is to obtain humic materials with low ash content, which has a low concentration of cations associated with the humic substance structure. These cations play a role in the secondary and tertiary structure of humic acid, so their elimination in the purification process could produce changes in the structure of the humic substances that modify the interaction of humic acid with other solutes [*von Wandruszka et al.,* 1997*; von Wandruszka,* 1998].

Fractionation Methods

Fractionation allows having a more uniform material in terms of molecular weight. Several methods have been used for fractionation of humic materials based on the physicochemical characteristics of these materials. The main characteristics used are solubility at different pH, molecular size, charge characteristic and adsorption [*Swift,* 1996]. While fractionation could provide valuable information, there are some concerns because the methods used for this purpose could change the structure of the humic materials [*Gaffney et al.,* 1996a].

The classic fractionation of the humic substances based in its solubility at different pH allows obtaining three fractions; humic acids, fulvic acids, and humin. Fulvic acid is soluble at all pH, in contrast humic acid which is insoluble at pH lower than 2 and humin is insoluble at all pH. This operational definition of humic material has proved

to be not very useful in the study of the interaction of these materials with solutes because each of these fractions represent a large and heterogeneous group of molecules.

Ultrafiltration is a simple and cheap technique that fractionates the humic substances with a series of membranes [*Swift,* 1985*; Wershaw and Aiken,* 1985*; Ambles,* 2001]. This technique permits processing large volume samples with little chemical alteration [*Gaffney et al.,* 1996a]. The main mechanism for the separation process is the selective sieve through the membrane; the molecule rejection is due to molecular size and shape, diffusion properties of the molecule in the fluid and the pore membrane; electrostatic and van der Waals interaction between the molecule and the membrane [*Kllduff and Weber,* 1992]. The manufacture provides a nominal molecular weight cutoff (NMWC), normally calibrated with globular molecules of known molecular weight. However, this calibration does not necessarily represent the size of the humic acid molecules, and in fact, many times overestimate the real size of the molecules. The solution-chemistry (pH and ionic strength) plays a vital role in the membranes performance, because the structure and surface charge of humic acids are dependent on the pH and the ionic strength of the solution [*Kllduff and Weber,* 1992]. For instance, humic-acid-fractions obtained with ultrafiltration membranes between 100 and 300 kDa have produced humic acids of 3.6 kDa determined by High Pressure Size Exclusion Chromatography (HPSEC). [*Li et al.,* 2004].

A variation of the method is hollow-fiber or tangential ultrafiltration. In this method the separation process is made by passing a solution through a membrane

that is parallel to the flow. This method has been used by some researchers to obtain fractions of different size that were further characterized by other analytical methods [*Gaffney et al.,* 1996a*; Kammer and Föstner,* 1998*; Christl et al.,* 2000].

The fractionation based on characteristic charges is made through electrophoresis that separates the sample base on the mobility of the charged molecules in an electric field. If the fractionation is made in a gel medium, the fractionation is obtained as a function of the size and the charge density of the molecule. The movement of the molecule in the gel is proportional to the charge density and inverse to the molecule size [*Swift,* 1985*; Swift,* 1996*; Senesi and Loffredo,* 2001].

Adsorption of humic acids is another method used to obtain different fractions. Several materials have been used as adsorbent, such as charcoal, alumina and methylmethacrylate resin XAD-8 [*Senesi and Loffredo,* 2001]. The XAD-8 resign has been extensively used [*Gu et al.,* 1996a*; Gu et al.,* 1996b*; McCarthy,* 2001], and with this material it is possible to obtain six different fractions; Hydrophobic-Based Fraction, Hydrophobic-Acid Fraction, Hydrophobic-Neutral Fraction, Hydrophilic-Base Fraction, Hydrophilic-Acid Fraction and Hydrophilic-Neutral Fraction. A detailed description of the methodology can be found in *Leenheer* [1981].

Characterization Methods

The analysis method most used for the study of molecular size and shape are gel-chromatography and other similar methodologies such as High Pressure Size Exclu-

sion Chromatography (HPSEC) and Size Exclusion Electrochromatography- Polyacrylamide Gel Electrophoresis (SEC-PAGE), Field Flow Fractionation (FFF), electromicroscopy, Small Angle X-ray Scattering (SAXS), and light scattering [*Senesi and Loffredo,* 2001]. The primary methods used for determination of functional group in humic substances are Pyrolysis Gas Chromatography and spectroscopic methods primarily the Fourier Transform Infrared Spectroscopy (FT-IR) and Nuclear Magnetic Resonance (NMR) [*Ambles,* 2001].

Field Flow Fractionation (FFF) is a technique to study the molecular size of the humic material, where the separation is based in the differences of diffusion-coefficients [*Beckett et al.,* 1987]. This method consists of the flow of a sample through a ribbon-shaped channel whose walls are semipermeable and parallel to the sample's flow. A laminar flow moves the molecules at a different velocity depending on the vertical position of the molecules. A cross-flow field is applied through a semipermeable membrane perpendicular to the laminar flow in such a way that the humic acid molecules are driven to the lower wall. This force is opposite to the diffusion of the macromolecules that set large molecules close to the lower wall (small diffusion coefficient) and to lower velocity; and small molecules close to the center of the laminar flow where the flow velocity is higher [*Beckett and Hart,* 1993*; Jones and Bryan,* 1998]. The separated molecules are measured through different detectors, such as UV-VIS or fluorescence spectrometer. In some way the instrument resembles an HPLC instrument.

This method requires a molecular weight calibration for the determination of the

size of the humic colloids. The standard should have similar molecular configuration as the humic acids. Polystyrene sulfonic acid standard (PSS) have been chosen for the calibration curve for humic acids because PSS has similar conformation as the humic acids, and PSS can be produced in very uniform molecular weight [*Beckett and Hart,* 1993*; Thang et al.,* 2001].

Humic acids are analytically measured by the amount of Dissolved Organic Carbon (DOC) found in a sample. DOC is related to the DOM by the amount of carbon present in the organic colloids. *Khan and Tomson* [1990] used the relationship DOM =1.724 DOC in the study of the influence of DOM in the transport of hydrophobic compounds. Other authors had reported the results of their research in terms of the amount of DOC present in the samples [*Enfield et al.,* 1989*; Spurlock and Biggar,* 1990*; Magee et al.,* 1991*; Lafrance et al.,* 1994*; Ding and Wu,* 1997*; Nelson et al.,* 1998*; Worrall et al.,* 1999].

4.4 Materials and Methods

4.4.1 Silica Sand and Sand Pretreatment

Silica sand (J.T. Baker, Phillipsburg, NJ; CAS N_0 14808-60-7) was dry sieved to obtain a material with particle size between 0.425 mm and 0.500 mm. The sand was cleaned by treating it with H_2O_2 to remove organic matter [*Kunze and Dixon,* 1986] and citrate-dithionite [*Holmgren,* 1967] to remove iron oxides. After the treatments, the

sand was extensively rinsed with deionized water and oven dried at 110°C.

4.4.2 Aluminosilicate Coating of Silica Sand

Three clay minerals, Texas Smectite (STx-1) and Georgia Kaolinite (KGa1) from the clay mineral repository (University of Missouri), and Illite No 36 from Morris, Illinois (Ward's Natural Science, Rochester, NY) were selected to be coated on the silica sand surface. The clays were treated to remove carbonate by the sodium acetate buffer method [*Kunze and Dixon,* 1986], organic matter by the H_2O_2 method [*Kunze and Dixon,* 1986], and iron oxides by the citrate-dithionite method [*Holmgren,* 1967]. Then, the clays were fractionated to obtain minerals smaller than 2 μm by the sedimentation method. The clays were converted to homoionic specimen by treating the Texas Smectite with 0.5 M $CaCl_2$, Georgia Kaolinite with 1M NaCl and Illite with 1 M KCl [*van Olphen,* 1977]. The clay coating was done using the PVA method described in detail in Chapter 2 of this dissertation.

Scanning electron microscopy (SEM) was performed using a Hitachi S520 microscope. Samples were mounted dry and sputtered-coated with a 10-15 nm gold layer. SEM analyses were performed before and after the column experiments to evaluate changes on the clay coated sand. Specific surface areas were determined on oven dried samples by N_2 adsorption and fitting a BET isotherm (ASAP2010, Micromeritics, Norcross, GA). The amount of clay coated on the silica grains was determined by detaching and measuring the amount of detached clay. The clay-coated sands were

immersed in a pH 7 solution and sonicating six times for 45 minutes in intervals of 3 to 4 hours. These procedures removed the clay coating effectively, as verified by microscopy. The amount of detached clay was quantified gravimetrically.

4.4.3 Humic Acid Material

Humic acid was obtained from Aldrich (Lot No. 03130JS). The humic acid was dissolved in double distilled water at pH 10 and stirred over night in a nitrogen atmosphere. Then the pH of the solution was dropped to pH 1 by adding 2 M HCl. The material was centrifuged and the supernatant was discarded. This procedure was repeated tree times. Then the humic acid was resuspended in a solution at pH 7. The humic acid concentration was determined using a UV-VIS spectrometer (HP 8452A, Hewlett Packard) at a wavelength of 254 nm. The spectroscopic measurements were calibrated with a TOC analyzer (TOC 5000, Shimadzu Corporation, Kyoto, Japan).

Humic acid was fractionated to reduce the polydispersivity of the sample. The fractionation was carried out using a hollow fiber filter (A/G technology Corporation, Needham, MA). The system consisted of peristaltic pump (Ismatec, Switzerland), two pressure transducers (Omega, model PX26, Stamford, CT), one at the inlet and one at the outlet of filter measuring the pressure of the sample, a data logger (C23X, Campbell Scientific, Logan, UT), the hollow fiber cartridge, and a set of valves to control the flux direction (Figure 4.2). The pressure of the system was controlled by the peristaltic pump. The humic acid was passed through four hollow fiber filters

of nominal molecular weight cut-off of 100, 50, 30, and 10 KDa. The humic acid concentration was $\approx$ 1.2 g/L organic carbon. The solution used for the hollow fiber fractionation was 0.1 M NaCl, to reduce the interaction of the humic acid with the filter membrane [*Klldu*ff *and Weber,* 1992]. After fractionation, humic acids were dialyzed at room temperature (20–22°C) until the electrical conductivity of the solution was less than 5 μS/m, using a cellulose ester membrane of NMWCO of 500 (Spectrum, CA).

The size distribution of humic acid samples were determined with an asymmetrical Field Flow Fractionation (Postnova analytics, Salt Lake City, Utah) with a UV detector. The instrument was calibrated with polystyrene sulfonic acid standard (PSS) of 4.6, 18.0, and 36.0 KDa (Polysciences, Warrington, PA). The standards and the samples were run with a solution at the same ionic strength and pH than used in the column experiments (pH 7.5 and 18.55 mM).

Sorption isotherms were determined for humic acids of the 10–30 KDa fraction on smectite, kaolinite, and illite coated sand. Clay-coated sands were equilibrated with a series of humic acids concentrations. Specifically, 0.5 g of clay-coated sand were equilibrated with 5 mL humic acids solution. The humic acids concentrations ranged from 0 to 180 mg/L OC, at pH 7.5$\pm$0.2 and ionic strength of 18.55 mM (same than column experiments). The humic acid-clay coated sand was then agitated on an orbital shaker for 24 h at room temperature (20 °C). The humic acid concentrations, expressed as organic carbon, in the liquid phase were determined by UV/VIS spectrometry (HP

8452A, Hewlett-Packard) at wavelengths of 254 nm. The amount of humic acid sorbed onto the clay-coated sand was calculated based on mass balance considerations. Even though the sorption isotherm was determined for the clay-coated sand the results are reported also based on the clay content of the coated sand only to compare with other published data.

4.4.4 Column Transport Experiments

Column experiments were performed in a borosilicate glass column of 1.0 cm diameter and 8 cm length (Omnifit, England). The column was packed with clean and clay-coated sand, in small increments of the porous materials, keeping the column always in a saturated condition. The background solution was pumped from the bottom with a peristaltic pump (Ismatec, Switzerland). To avoid the presence of air bubbles, the column was filled with CO_2 gas for about one minute. After the column was packed at least 20 pore volumes were pumped through the column to dissolve any residual CO_2 gas bubbles that could remain in the column.

The background solution was a mixture of ions to mimic a soil solution composition; 4.45 mM $CaCl_2$, 1.4 mM $MgCl_2$, 0.4 mM KCl, 0.7 mM and NaCl, with an ionic strength of 18.55 mM. Sodium nitrate ($NaNO_3$, 0.2 mmol) was used as conservative tracer in all the column experiments. The tracer and humic acid concentration were measured online with a diode array spectrometer (HP 8452A, USA); nitrate was measured at 220 nm and humic acids at 254 nm. Calibrations of tracers standards followed Beer's

law (Figure 4.1).

Column experiments were analyzed using the code Hydrus 1-D [*Šimůnek et al.*, 1998]. The tracer experiments were used to determine the hydrodynamic dispersion coefficient D using the advection-dispersion equation (ADE). The Peclet number, Pe, was then calculated as $Pe = vL/D$, where L is the length of the column.

$$\Theta\frac{\partial C}{\partial t} + \rho\frac{\partial S}{\partial t} = D\frac{\partial^2 C}{\partial x^2} - v\frac{\partial C}{\partial x} \tag{4.1}$$

where $\partial S/\partial t$ is the sorption term. Hydrus 1-D implements the general sorption equation

$$S_k = \frac{k_{s,k}C_k^{\beta_k}}{1 + \eta_k C_k^{\beta_k}} \tag{4.2}$$

where $k_{s,k}$ [L^3M^{-1}], βk [-] and μ_k [L^3M^{-1}] are empirical coefficients. Freundlich and Langmuir isotherm are obtained when the proper values are set for the coefficients, e.g., when β_k =1 the general isotherm becomes the Langmuir isotherm, when η_k=0, the equation becomes a Freundlich isotherm. In addition to the general sorption isotherm, the model includes a first-order term for irreversible sorption. Including all the parameters the $\partial S/\partial t$ can be written as:

$$\frac{\partial S}{\partial t} = \Big(\frac{k_{s,k}C_k^{\beta_k}}{1 + \eta_k C_k^{\beta_k}}\Big) + \mu_k \tag{4.3}$$

The modeling was used in the inverse mode to obtain parameters of the sorption coefficients of the humic acids on the clay-coated sand, as well in direct modeling mode

using the parameters determined in the humic acid sorption isotherm.

4.5 Results and Discussion

4.5.1 Clay Coating

The clay content of the clay-coated sand was determined at the beginning and at the end of the columns transport experiments (Table 4.1). The amount of clay remaining in the column was higher than 90% of the initial clay content, except for the high-load smectite that a higher detachment was observed. The SEM micrograph of the clay-coated sand showed uniform and stable coverage of the clay at the sand surface (Figure 4.3). No evident change was observed after the humic acid-column-transport experiments were performed.

4.5.2 Humic Acid Fractionation

The fractograms of the polystyrene sulfonic acid standards are shown in Figure 4.4a. The standards had a clear pick at different elution times depending on the size of the molecules. The elution time was independent of the molecule concentration but the size of the peak was dependent on the polystyrene sulfonic acid concentration. The field-flow fractionation calibration was linear with a high coefficient of correlation (Figure 4.4b). This is similar to previously reported data [*Klldu*ff *and Weber*, 1992].

The humic acid fractionation reduced the polydispersivity of the sample (Figure

4.5). However the different hollow fiber filters did not produce fractions of different sizes. This is probably due to the ionic strength of the background solution used in the fractionation procedure. This concentration was chosen to reduce the interaction between the humic material and the membrane based on a previous report [*Kllduff and Weber,* 1992]. However, for the specific filter used in this study, the ionic strength seemed to be too high to produce a separation of the humic acids molecules. It has been reported in the literature that this type of membrane tends to interact with the humic material, producing an overestimation of the humic size [*Li et al.,* 2004]. In fact, the nominal molecular weight of the membranes were several times higher than the actual humic acid size, as determined by the field flow fractionation. Since the humic acid fractionation did not produce different humic acids fractions, only the humic material obtained from the 10-30 KDa hollow fiber was used to run the humic acid breakthrough curves.

The sorption of humic acid on aluminosilicate clays is shown in Figure 4.6. The humic acid isotherms were conducted in clay coated sand. To make possible the comparison of our results with others reported sorption isotherms, the isotherms are also reported in terms of the clay minerals present on the sand surface. Similarly, the amount of humic acid sorbed is shown in terms of the surface are of the clay-coated sand (Table 4.1). *Chorover and Amistadi* [2001] found sorption around 12 mg OC/g of montmorillonite using a Wyoming smectite (Swy-2) with a humic acid obtained from a forest soil. Kaolinite sorption ranged between 0.8 and 2.5 mg OC/g clay depending on

the origin and surface charge of the humic acid, at similar pH than used in this study [*Saada et al.,* 2003]. The sorption of the humic acid in base on the surface area of the clay-coated sand reduced the difference between minerals that agree with previous reports [*Chorover and Amistadi,* 2001]

4.5.3 Humic Acid Breakthrough

The breakthrough curves of NO_3^- were similar among the clay-coated sands. Only the high load shown an early breakthrough due to the anion exclusion, that is in agreement to what was found in chapter 3 (Figure 4.7). The humic acid breakthrough curves are shown in Figure 4.8. The humic acids breakthrough curves were well reproducible (Figure 4.9).

The porous media had clear differences in the capacity to sorb humic acids. In the short humic acids injection experiments, illite-coated sand had the highest capacity to sorb humic acids of all the clay used. This is not in agreement with the result of the batch isotherm, which showed that smectite clay had the highest sorption affinity (but illite-coated sand has the highest specific surface area). The behavior of the low-coated smectite (16.7 mg clay/g sand) and kaolinte (33.5 mg clay/g sand) are qualitatively in agreement of previously reported sorption of both clays, in which smectite had higher capacity due to the higher surface area [*Baham and Sposito,* 1994].

We conducted a set of experiments in illite and high-load-smectite-coated sand with longer pulse of humic acids. The two clays were chosen because they had the high-

est sorption affinity for humic acid. The injection of approximately 10 mg OC/L for 64-pore volume on illite-coated sand and 86 pore volume on high-load-smectite-coated sand, demonstrate the differences between the two porous media. Both clay-coated sands showed a maximum humic acid breakthrough around 40% of the initial concentration. However, the shape of the curves were quite different: whereas illite-coated sand showed a quick and steep initial breakthrough, smectite-coated sand showed an initial lag in humic acid breakthrough. The second injection of humic acid produced steeper breakthrough of humic acids in both clay-coated sand. This increasing steepness of the initial breakthrough link for sequential injections of humic acids has also been observed in iron-coated sand [*Dunnivant et al.*, 1992]. The second injection demonstrated that sorption site on the clay surfaces are limited. The different shape of the breakthrough curves could be explained in base to previous studies. *Chorover and Amistadi* [2001] reported that smectite clay did not make a large distinction between the humic acid molecules of different molecular weight, therefore the bulk humic acid was sorbed on the clay surface. This could explain the longer time it took to reach a relative stable breakthrough. In contrast, illite could present a similar response than reported for kaolinite, with preferential sorption for large molecules with low surface charge. This response could explain the early and quick breakthrough observed in this porous medium [*Balcke et al.*, 2002]. However there is no evidence in the literature that illite-humic acid interaction had this pattern. One concern is that the clay-coating with PVA produced a reduction in the hydrophilicity of the clay that could influence

the response of the porous media, enhancing the interaction of the clay with the less hydrophilic humic acid fraction.

In base of previous report is very likely that the early breakthrough of humic acid was due to the fast movement of humic acids of low-molecular weight and higher surface charge [*Gu et al.,* 1996a*; Balcke et al.,* 2002]. The surface charge of clays and humic acids could produce an anion exclusion that could explain the fast breakthrough observed in our experiments.

4.5.4 Humic Acid Breakthrough Modeling

The Peclet number of the model humic acid breakthrough demonstrated that the porous media had similar hydrodynamic properties (Table 4.2).

The modeling of the humic acid breakthrough curves are shown in Figure 4.11. The modeling of the experimental data using the sorption-isotherm parameter did not represent well the data observed. When the inverse mode was used, a first order irreversible sorption parameter should be included to represent the maxima breakthrough observed (Table 4.2). This term represents irreversible sorption due to physical constrain in the column. The irreversible sorption parameter could not be obtained from the batch isotherm, therefore this is one of the main reasons why the modeling using the batch-sorption parameter did not result in a good representation of the data. The best-modeled breakthrough curve was the long injection humic acid on illite-coated sand. In the smectite- and kaolinite coated-sand the estimated values were far from

the observed data. When the Langmuir-type of isotherm was used, the model did not converge.

4.6 Conclusions

Humic acid transport was affected by the type of clay coated on the silica sand surface. Kaolinite was less effective to sorbed humic acids than smectite- and illite-coated sands. Humic acid was able to breakthrough around 40% of the initial humic acid concentration on illite-coated sand and high-load-smectite-coated sand. A significant fraction of the humic acid was able to move quickly through the porous media. The simulation of the humic acid breakthrough using the isotherm sorption parameter predicted that breakthrough of humic acid should reach 100% of the initial concentration. The difference between the predicted and observed humic acid breakthrough showed that more complex interaction occurred between the clay minerals and the humic acid. A better fit was obtained when a first order irreversible sorption term was included in the model. It was demonstrated that humic acids can move trough a clay-dominated porous media. Further research should be carried out to evaluate if humic acid movement occurs in natural environments.

4.7 Tables and Figures

Table 4.1: Clay-coverage of sands used in the experiments.

Clay coated sand	Initial Coverage mg clay/ g sand	Final Coverage mg clay/ g sand	Specific Surface Area m^2/g
Clean sand	–	–	0.04±0.001
Kaolinite (KGa1)	33.5±0.3	31.3±0.6	0.74±0.01
Illite (No. 36, Morris)	39.8±1.4	34.3±0.3	1.8±0.02
Smectite-(STx1) (low load)	15.7±1.6	14.5±1.7	1.1±0.003
Smectite-(STx1) (high load)	31.1±1.4	26.9±2.1	1.5±0.01

errors are one standard deviation (n=3)

Table 4.2: Parameter obtained from modeling humic acid breakthrough curves

Clay coated sand	D	Pe	Kd	β	μ_k	r^2
	cm^2/min	mL/g		–	min^{-1}	
Clean sand	0.139	37.8	0.028	4.59	0.069	0.88
Kaolinite (KGa1)	0.151	36.9	0.12	7.63	0.31	0.84
Illite (No. 36, Morris)	0.141	39.6	0.069	2.35	0.27	0.93
Smectite-(STx1) (high load)	0.148	35.6	55.9	0.06	0.29	0.81

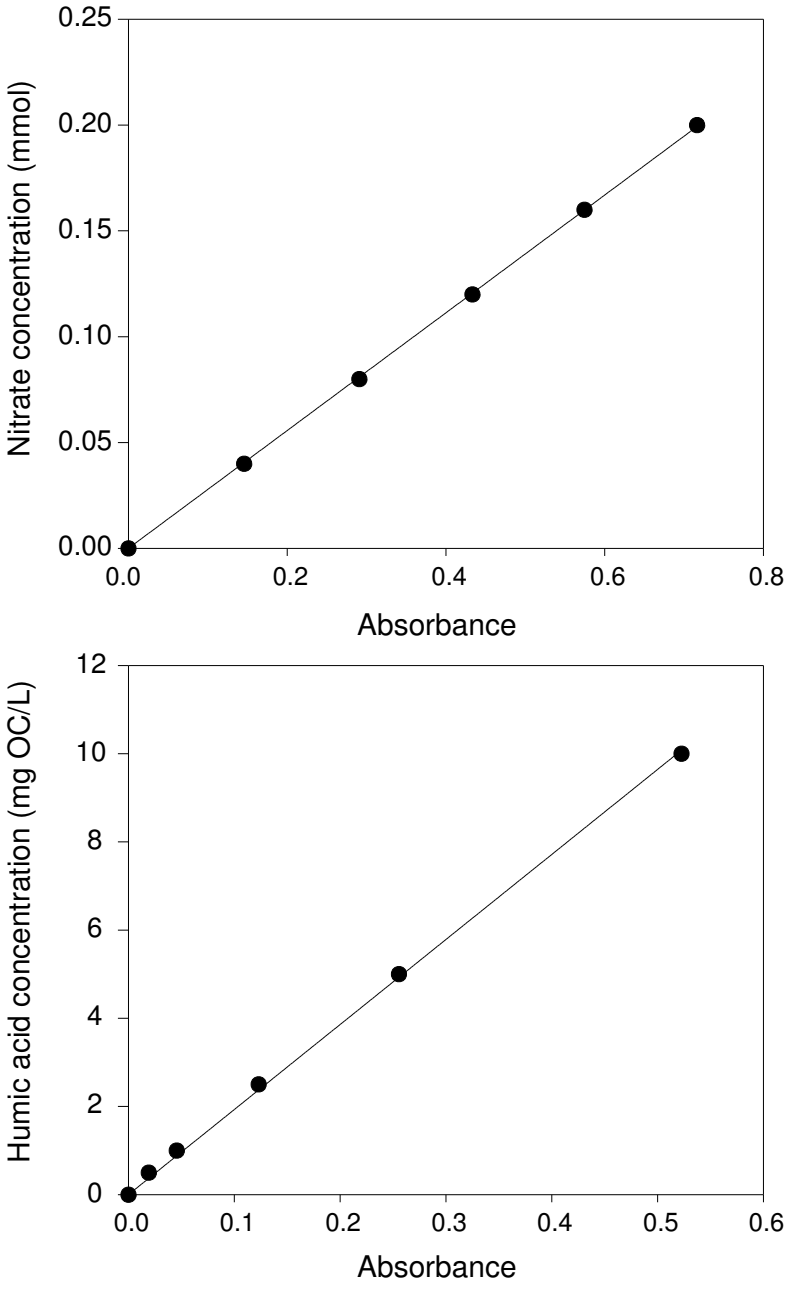

Figure 4.1: UV-VIS calibration curves for nitrate and humic acids.

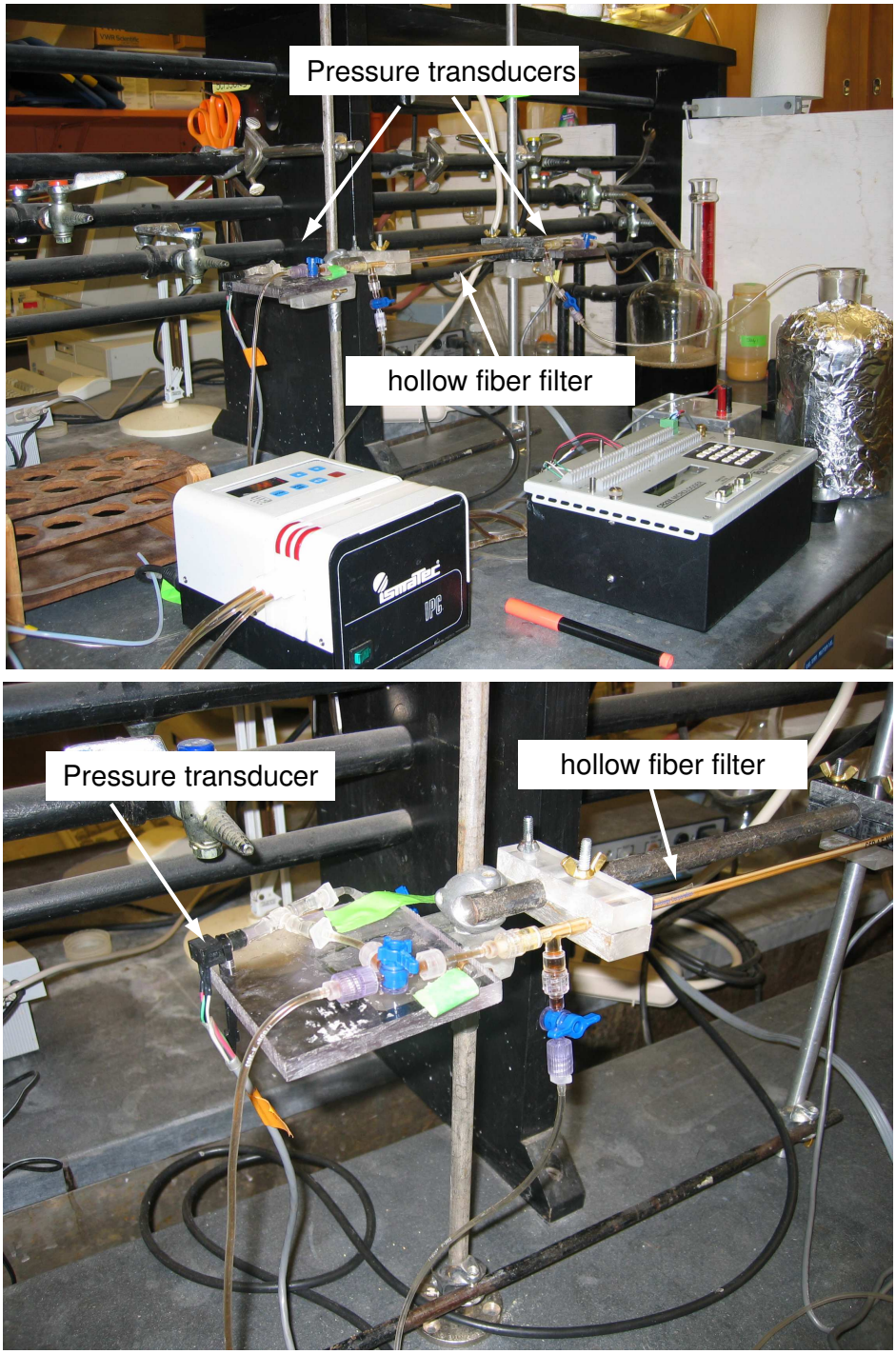

Figure 4.2: Set-up of hollow fiber fractionation system.

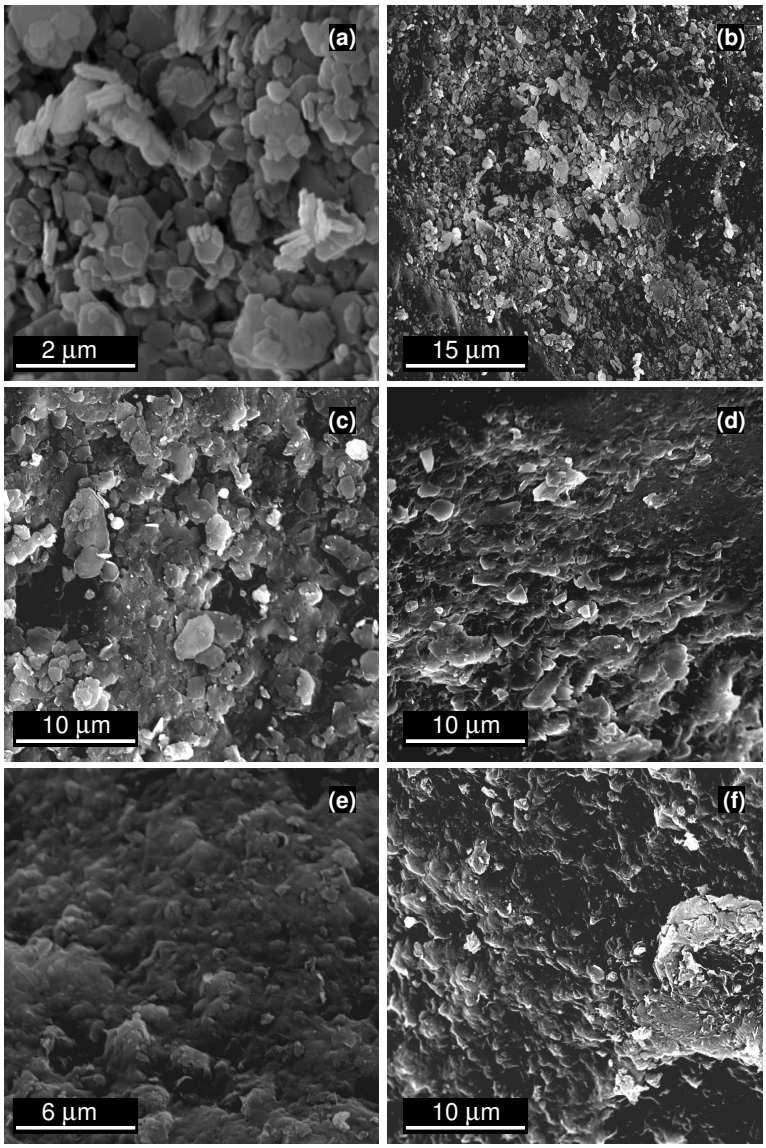

Figure 4.3: Scanning electron micrographs of (a, b) kaolinite-coated sand (KGa1), (c, d) illite-coated sand (No. 36, Morris), and (e, f) smectite-coated (STx1) sand. The left column (a,c,e) shows clays-coated sands before humic acid column experiments, and (b,d,f) shows clays-coated sands after humic acid column experiments.

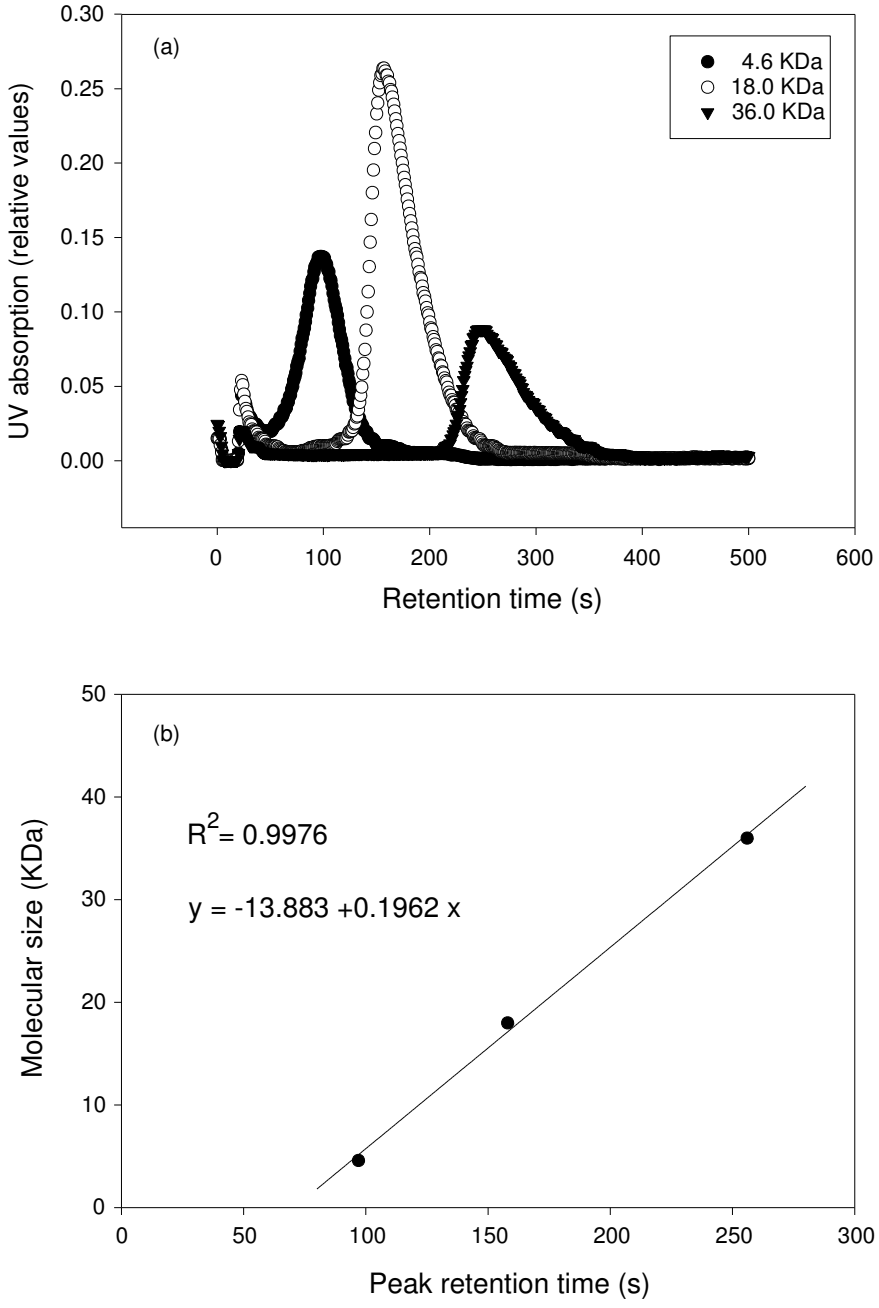

Figure 4.4: Calibration of fractionation system with polystyrene sulfonic standard (PSS).

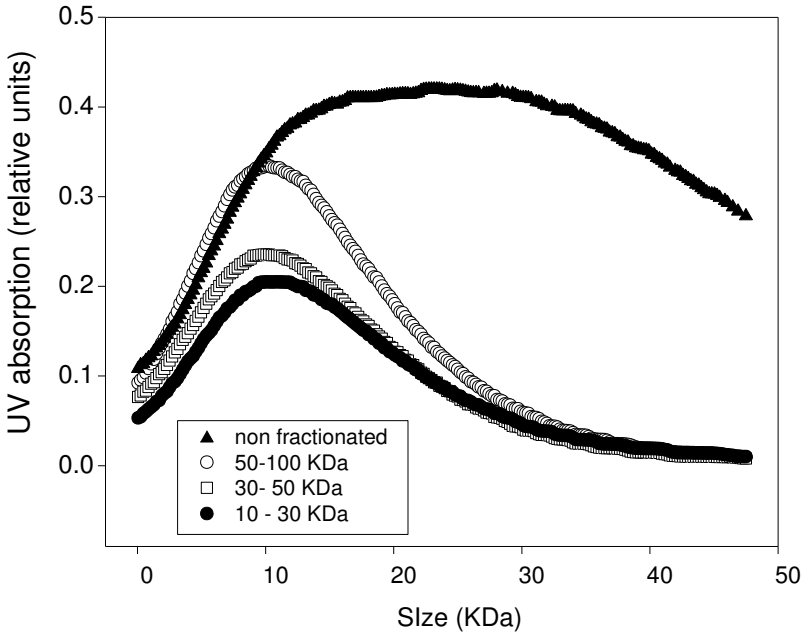

Figure 4.5: Size fractions of humic acids fractionated by filtration. Size fractions were measured with field flow fractionation.

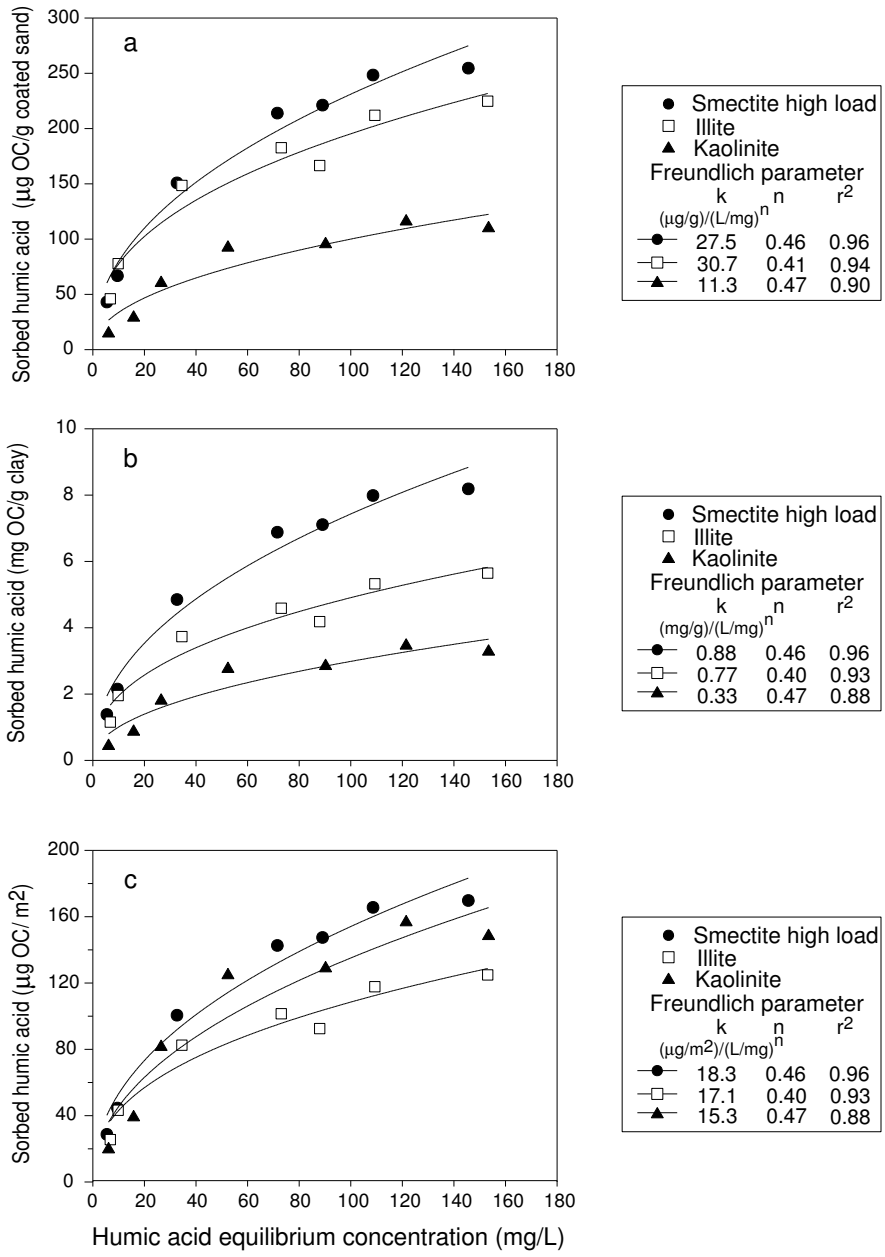

Figure 4.6: Humic acid isotherms on clay-coated sands. (a)Humic acid isotherm on clay-coated sands (b)isotherm express in term of clay minerals content of clay-coated sands (c) isotherm express in term of surface area of clay-coated sands.

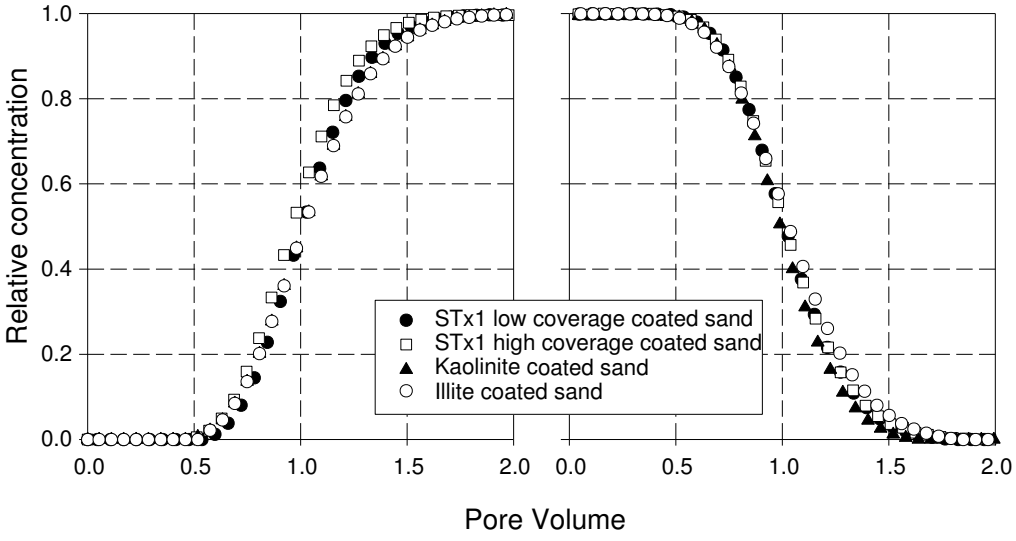

Figure 4.7: Tracer (nitrate) breakthrough curves on clay coated sand.

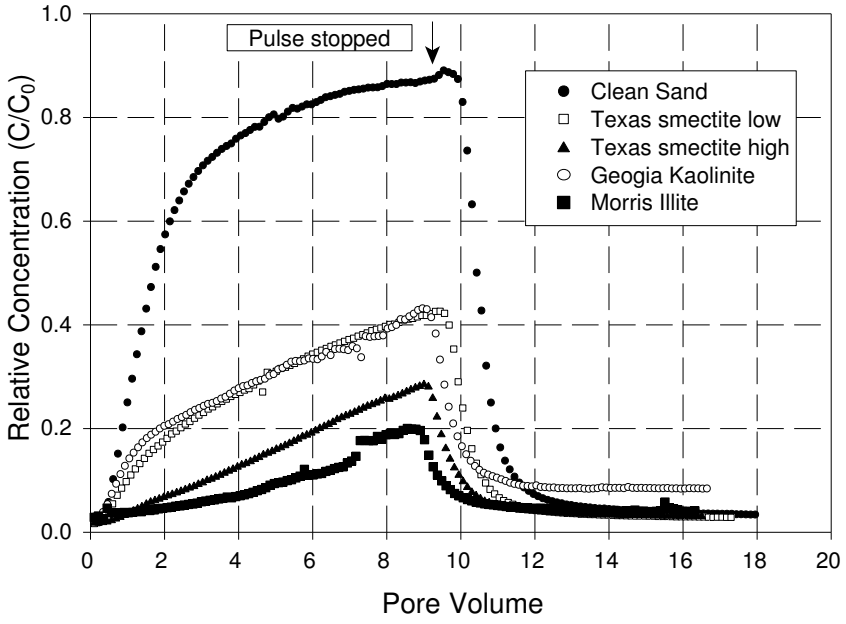

Figure 4.8: Humic acid breakthrough curves in clay-coated sand.

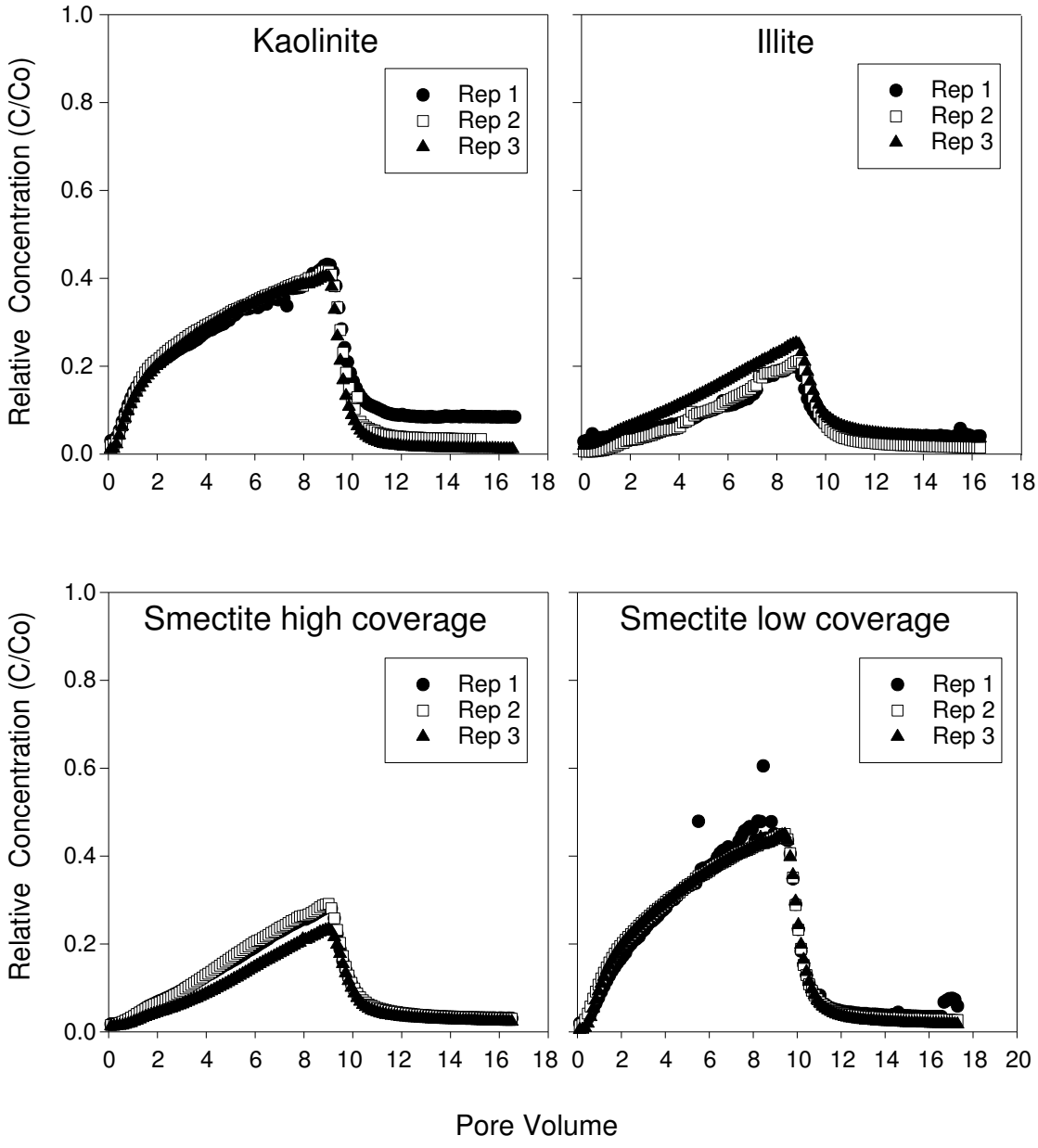

Figure 4.9: Reproducibility of humic acid curves in clay-coated sand.

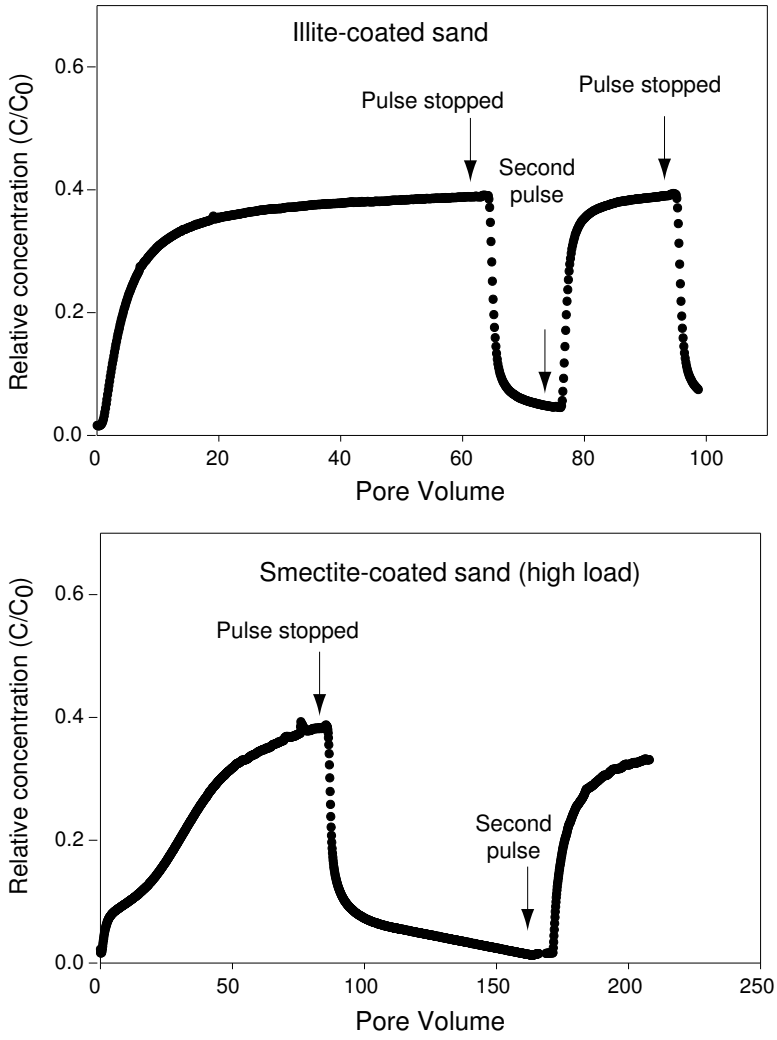

Figure 4.10: Humic acid breakthrough curves on clay coated sand.

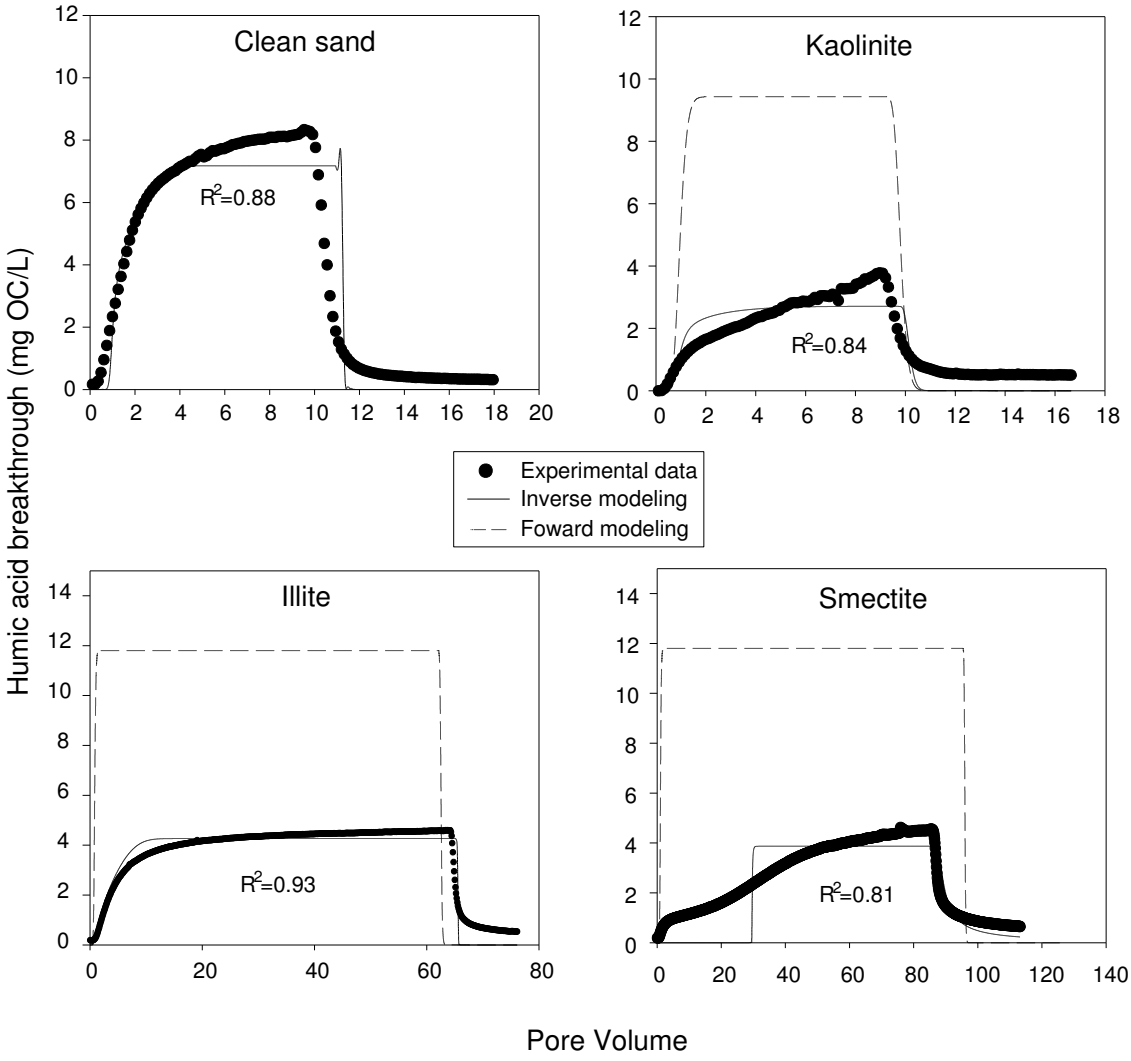

Figure 4.11: Modeling of humic acid breakthrough curves.

Chapter 5

Summary and Conclusion

We developed a new methodology to immobilize aluminosilicate clays on inert supports like silica sand. Clay minerals are important components of soil and sediments and play an important role in the transport of solutes. The study of the transport of solutes in clayey systems is challenging due to the inherent low hydraulic conductivity of the clays [*Wibulswas*, 2004]. The research described in this dissertation followed approaches reported earlier on the coating of silica sand with iron oxides [*Chao and Harward*, 1964; *Scheidegger et al.*, 1993; *Hur and Schlautman*, 2003]. We used two polymers to bind clay minerals to silica sand: polyacrylamide and polyvinyl alcohol. Three aluminosilicate clays, Texas smectite (STx1), Georgia kaolinite (KGa1), and Morris illite were used. The stability of the clay-coated sands was determined over a pH range of 3 – 13 and in long-term flow experiments. The clay immobilized with polyvinyl alcohol had high stability with a minimum amount of clay detached from the silica sand. Alternatively, when polyacrylamide was used the coated clay presented a pH dependent stability with high clay detachment at pH $>$ 9. We studied the

electrophoretic mobility of the natural and clay-polymer complexes and we found small differences between the natural clay and the clay-polymer composite. In addition, the immobilized clay minerals had a similar isoelectric point as the clay minerals themselves. The thermodynamic properties of the clays demonstrated that the illite-polymer complex increased the electron acceptor component of the surface tension, and decreased the wettability of the clay. The PVA-smectite complex had smaller wettability than the smectite clay, but for PAM, no differences between polymer-clay and clay were found.

We used humic acid-, ferrihydrite-, and aluminosilicate clay-coated silica sand to study miscible transport of a conservative tracer. The miscible displacement experiments were modeled with CXTFIT and we found that all the porous materials had similar hydrodynamic properties. We also found that the nitrate tracer was subject to size exclusion on the clay-coated sand and the magnitude of the effect was proportional to the clay content.

Finally, we used the clay-coated silica sand to study thransport of humic acids as affected by clay mineral type. Column experiments were conducted using Aldrich humic acid and a porous media with kaolinite, illite, and smectite coated on silica sand. The humic acid was injected into the column at a concentration around 10 mg/L of organic carbon and pH 7.5. The background solution was a mixture of ions to mimic a soil solution. The clay-coated sand sorbed a large amount of the humic acid, but still a significant amount of humic acid moved through the column. The humic acid

breakthroughs were modeled using the Hydrus 1-D code in inverse mode [*Šimůnek et al.,* 1998]. The breakthrough data were used to determine the isotherm parameter to describe the transport of the humic acid. The Freundlich isotherm resulted in the best description for the humic acid breakthrough.

The main conclusions of this study are:

- It is possible to immobilize clay minerals on silica sand surfaces using polymers as bridging agents between the clay and silica surfaces.

- The polymers did not change the isoelectric point nor the electrophoretic mobility of the clay minerals. However, both polymers increased the electron donor component of the surface tension of illite and decrease the wettability of the clay. Similarly, polyvinyl alcohol increased the electron donor component of the surface tension of smectite and decrease the wettability of the clay. Polyacrylamide did not produce changes in surface thermodynamic properties of the smectite clay. Kaolinite thermodynamic properties were not affected by the polymers.

- It is possible to change sorption properties of silica sand by coating different clay minerals, iron oxides, or humic acids. The sorption property of the porous media was controlled by the coated minerals or humic acids. The hydrodynamic properties of the porous media was controlled by the silica sand. The Peclet number showed that the porous media with different coated materials presented similar hydrodynamic properties.

- Clay-coated sand sorbed large amount of humic acid. However, a significant amount of humic acid was able to move through clay-coated sand media. Consecutive humic acid injection produced a steepness in humic acid breakthrough.

Bibliography

Aiken, G. R., Isolation and concentration techniques for aquatic humic substances, in *Humic Substances in Soil, Sediment and Water. Geochemistry, Isolation and Characterization*, edited by G. Aiken, D. McKnight, W. R., and P. MacCarthy, pp. 363–385, John Wiley, New York, 1985.

Ake, C. L., K. Mayurana, G. R. Bratton, and T. D. Phillips, Development of porous clay-based composites for the sorption of lead from water, *J. Toxicol. Environ. Health A.*, *63*, 459–475, 2001.

Ake, C. L., K. Mayurana, G. R. Bratton, and T. D. Phillips, Porous organoclay composite for the sorption of polycyclic aromatic hydrocarbons and pentachlorophenol from groundwater, *Chemosphere*, *51*, 835–844, 2003.

Ambles, A., Methods to reveal the structure of humic substances, in *Biopolymers*, edited by M. Hofrichter, and A. Steinbuchel, pp. 325–348, Wiley-Vch, Weinheim, Germany, 2001.

Anderson, P. R., and M. M. Benjamin, Effects of silicon on the crystallization and adsorption properties of ferric oxides, *Environ. Sci. Technol.*, *19*, 1048–1053, 1985.

Aras, A., The change of phase composition in kaolinite- and illite-rich clay-based ceramic bodies, *Appl. Clay Sci.*, *24*, 257–269, 2004.

Argillier, J. F., A. Audibert, J. Lecourtier, M. Moan, and L. Rousseau, Solution and adsorption properties of hydrophobically associating water-soluble polyacrylamides, *Colloids Surf. Physicochem. Eng. Aspects*, *113*, 247–257, 1996.

Baham, J., and G. Sposito, Adsorption of dissolved organic carbon extracted from sewage sludge on monmorillonite and kaolinite in the presence of metal ions, *J. Environ. Qual.*, *23*, 147–153, 1994.

Bajpai, A. K., and N. Vishwakarma, Adsorption of polyvinylalcohol onto Fuller's earth surfaces, *Colloids Surf. Physicochem. Eng. Aspects*, *220*, 117–130, 2003.

Balcke, G., N. Kulikova, S. Hesse, F. Kopinke, I. Perminova, and F. Frimmel, Adsorption of humic substances onto kaolin clay related to their structural features, *Soil Sci. Soc. Am. J.*, *66*, 1805–1812, 2002.

Beckett, R., and B. T. Hart, Use of field-flow fractionation techniques to characterized aquatic particles, colloids and macromolecules, in *Environmental particles. Volume 2*, edited by J. Buffle, and H. P. v. Leeuwen, pp. 165–205, Lewis Publishers, Boca raton, Fl, 1993.

Beckett, R., Z. Jue, and J. C. Giddings, Determination of molecular weight distributions of fulvic and humic acids using flow field-flow fractionation, *Environ. Sci. Technol.*, *21*, 289–295, 1987.

Benjamin, M. M., R. S. Sletten, R. P. Bailey, and T. Bennett, Sorption and filtration of metals using iron-oxide-coated sand, *Water Res.*, *30*, 2609–2620, 1996.

Borden, D., and R. F. Giese, Baseline studies of the Clay Minerals Society source clays: Cation exchange capacity measurements by the ammonia-electrode method, *Clays Clay Miner.*, *49*, 444–445, 2001.

Bortiatynski, J. M., P. G. Hatcher, and H. Knicker, NMR techniques (C, N and H) in studies of humic substances, in *Humic and Fulvic Acids: Isolation, Structure, and Environmental Role*, edited by J. Gaffney, N. Marley, and S. Clark, pp. 57–77, American Chemical Society, Washington, DC, 1996.

Bowman, R. S., Evaluation of some new tracers for soil water studies, *Soil Sci. Soc. Am. J.*, *48*, 897–993, 1984.

Chao, T. T., and S. C. Harward, Iron or aluminium coating in relation sulfate adsorption characterstic of soils, *Soil Sci. Soc. Am. Proc.*, *28*, 632–635, 1964.

Chiou, C. T., R. L. Malcolm, T. I. Brinton, and D. E. Kile, Water solubility enhancement of some organic pollutants and pesticides by dissolved humic and fulvic acids, *Environ. Sci. Technol.*, *20*, 502–508, 1986.

Chorover, J., and M. Amistadi, Reaction of forest floor organic matter with goethite, birnesite and smectite surfaces, *Geochim. Cosmochim. Acta*, *65*, 95–109, 2001.

Christl, I., H. Knicker, I. Kogel-Knabner, and R. Kretzschmar, Chemical heterogeneity of humic substances: Characterization of size fractions obtained by hollow-fiber ultrafiltration, *Eur. J. Soil Sci.*, *51*, 617–625, 2000.

Clay, D. E., Z. Zheng, Z. Liu, S. A. Clay, and T. P. Trooien, Bromide and nitrate movement through undisturbed soil columns, *J. Environ. Qual.*, *33*, 338–342, 2004.

de Bussetti, S. G., and E. A. Ferreiro, Adsorption of poly(vinyl alcohol) on montmorillonite, *Clay Miner.*, *52*, 334–340, 2004.

De Paolis, F., and J. Kukkonen, Binding of organic pollutants to humic and fulvic acids: Influence of pH and the structure humic material, *Chemosphere*, *34*, 1693–1704, 1997.

Deng, Y., *Organic polymer-clay interaction and intercalation of kaolinite*, PhD thesis, Texas A & M University, 2001.

Ding, J. Y., and S. C. Wu, Transport of organochlorine pesticides in soil columns enhanced by dissolved organic carbon, *Water Sci. Technol.*, *35*, 139–145, 1997.

Dunnivant, F. M., P. M. Jardine, D. L. Taylor, and J. F. McCarthy, Transport of naturally occurring dissolved organic carbon in laboratory columns containing aquifer material, *Soil Sci. Soc. Am. J.*, *56*, 437–444, 1992.

Emerson, W. W., The effect of polymers on the swelling of montmorillonite, *J. Soil Sci.*, *14*, 52–63, 1963.

Emerson, W. W., and M. Raupach, The reaction of polyvinyl alcohol with montmorillonite, *Aust. J. Soil Res.*, *2*, 46–55, 1964.

Enfield, C. G., G. Bengtsson, and R. Lindqvist, Influence of macromolecules on chemical transport, *Environ. Sci. Technol.*, *23*, 1278–1286, 1989.

Engebretson, R., and R. von Wandruszka, The effect of molecular size on humic acid associations, *Org. Geochem.*, *26*, 759–767, 1997.

Faibish, R. S., W. Yoshida, and Y. Cohen, Contact angle study on polymer-grafted silicon wafers, *J. Colloid Interface Sci.*, *256*, 341–350, 2001.

Gaffney, J. S., N. A. Marley, and K. A. Orlandini, The use of hollow-fiber ultrafilters for the isolation of natural humic and fulvic acids, in *Humic and Fulvic Acids: Isolation, Structure, and Environmental Role*, edited by J. Gaffney, N. Marley, and S. Clark, pp. 25–40, American Chemical Society, Washington, DC, 1996a.

Gaffney, J. S., N. A. Marley, and S. B. Clark, Humic and fulvic acids and organic colloidal materials in the environment, in *Humic and Fulvic Acids: Isolation,*

Structure, and Environmental Role, edited by J. Gaffney, N. Marley, and S. Clark, pp. 2–16, American Chemical Society, Washington, DC, 1996b.

Graber, E. R., Z. Gerstl, E. Fisher, and U. Mingelgrin, Enhanced transport of atrazine under irrigation with effluent, *Soil Sci. Soc. Am. J.*, *59*, 1513–1519, 1995.

Greenland, D. J., Adsorption of poly(vinyl alcohols) by montmorillonite, *J. Colloid Sci.*, *18*, 647–664, 1963.

Gu, B., T. L. Mehlhorn, L. Liyuan, and J. F. McCarthy, Competitive adsorption, displacement, and transport of organic matter on iron oxide: I. Competitive adsorption, *Geochim. Cosmochim. Acta*, *60*, 1943–1950, 1996a.

Gu, B., T. L. Mehlhorn, L. Liyuan, and J. F. McCarthy, Competitive adsorption, displacement, and transport of organic matter on iron oxide: II. Displacement and transport, *Geochim. Cosmochim. Acta*, *60*, 2977–2992, 1996b.

Gu, G., Z. Zhou, Z. Xu, and J. H. Masliyah, Role of fine kaolinite clay in toluene-diluated bitumen/water emulsions, *Colloids Surf. Physicochem. Eng. Aspects*, *215*, 141–153, 2003.

Guo, L., J. B. Thomas, A. S. Felsot, and D. H. Thomas, Sorption and movement of alachlor in soil modified by carbon-rich waste, *J. Environ. Qual.*, *22*, 186–194, 1993.

Hajjaji, M., S. Kacim, and M. Boulmane, Mineralogy and firing characteristics of a clay from the valley of Ourika (Morocco), *Appl. Clay Sci.*, *21*, 203–212, 2002.

Hansen, B. O., P. Kwan, M. M. Benjamin, and G. V. Korshin, Use of iron oxide-coated sand to remove Strontium from simulated Hanford tank waste, *Environ. Sci. Technol.*, *35*, 4905–4909, 2001.

Haynes, M. H. B., Extraction of humic substances from soil, in *Humic Substances in Soil, Sediment and Water. Geochemistry, Isolation and Characterization*, edited by G. Aiken, D. McKnight, W. R., and P. MacCarthy, pp. 329–362, John Wiley, New York, 1985.

Haynes, M. H. B., Concepts of the origins, composition and structure of humic substances, in *Advances in Soil Organic Matter Research: The Impact on Agriculture and the Environment*, edited by W. S. Wilson, pp. 3–22, The Royal Society of Chemistry, Cambridge, UK, 1991.

Heath, D., and T. F. Tadros, Influence of pH, electrolyte, and poly(vinyl alcohol) addition on the rheological characteristics of aqueous dispersions of sodium montmorillonite, *J. Colloid Interface Sci.*, *93*, 307–319, 1982.

Holmgren, G. G. S., A rapid citrate-dithionite extractable iron procedure, *Soil Sci. Soc. Am. Proc.*, *31*, 210–211, 1967.

Hur, J., and M. A. Schlautman, Molecular weight fractionation of humic substances by adsorption onto minerals, *J. Colloid Interface Sci.*, *264*, 313–321, 2003.

James, R. V., and J. Rubin, Transport of chloride ion in a water unsaturated soil exhibiting anion exclusion, *Soil Sci. Soc. Am. J.*, *50*, 1142–1149, 1986.

Jones, M. N., and N. D. Bryan, Colloidal properties of humic substances, *Adv. Colloid. Interface Sci.*, *78*, 1–48, 1998.

Kammer, F. v. d., and U. Föstner, Natural colloid characterization using flow-field-flow-fractionation followed by multi-detector analysis, *Water Sci. Technol.*, *196*, 173–180, 1998.

Khan, A. T., and M. B. Tomson, Ground water transport of hydrophobic organic compounds in the presence of dissolved organic matter, *Environ. Toxicol. Chem.*, *9*, 253–263, 1990.

Kinniburgh, D. G., J. K. Syers, and M. L. Jackson, Specific adsorption of trace amounts of calcium and strontium by hydrous oxides of iron and aluminum, *Soil Sci. Soc. Am. Proc.*, *39*, 464–470, 1975.

Kllduff, J., and J. J. Weber, Transport and separation of organic macromolecules in ultrafiltration processes, *Environ. Sci. Technol.*, *26*, 569–577, 1992.

Kocherginsky, N. M., and J. W. Stucki, Supported clay membrane: a new way to characterize water and ion transport in clays, *Adv. Env. Res.*, *5*, 197–201, 2001.

Koopal, L. K., Y. Yang, A. J. Minnaard, P. L. M. Theunissen, and W. H. Van Riemsdijk, Chemical immobilization of humic acid on silica, *Colloids Surf. Physicochem. Eng. Aspects*, *141*, 385–395, 1998.

Kretzschmar, R., H. Holthoff, and H. Sticher, Influence of pH and humic acid on coagulation kinetics of kaolinite: A dynamic light scattering study, *J. Colloid Interface Sci.*, *202*, 95–103, 1998.

Kunze, G. W., and J. B. Dixon, Pretreatment of minerological analysis, in *Methods of Soil Analysis. Part 1. Physical and mineralogical analysis*, edited by A. Klute, pp. 91–100, Soil Sci. Soc. Am., Madison, WI, 1986.

Lafrance, P., L. Marineau, L. Perrault, and J. Villeneuve, Effect of natural organic matter found in groundwater on soil adsorption and transport of pentachlorophenol, *Environ. Sci. Technol.*, *28*, 2314–2320, 1994.

Laird, D. A.and Barriuso, E., R. H. Dowdy, and W. C. Koskinen, Adsorption of atrazine on smectites, *Soil Sci. Soc. Am. J.*, *56*, 62–67, 1992.

Laor, Y., C. Zolkov, and R. Armon, Immobilizing humic acid in a sol-gel matrix: A new tool to study humic-contaminants sorption interactions, *Environ. Sci. Technol.*, *36*, 1054–1060, 2002.

Leenheer, J. A., Comprehensive approach to preparative isolation and fractionation of dissolved organic carbon from natural waters and wastewater, *Environ. Sci. Technol.*, *15*, 579–587, 1981.

Leenheer, J. A., Fractionation techniques for aquatic humic substances, in *Humic Substances in Soil, Sediment and Water. Geochemistry, Isolation and Characterization*, edited by G. Aiken, D. McKnight, W. R., and P. MacCarthy, pp. 409–429, John Wiley, New York, 1985.

Li, L., Z. Zhaoa, W. Huang, P. Penga, G. Shenga, and J. Fua, Characterization of humic acids fractionated by ultrafiltration, *Org. Geochem.*, *35*, 1025–1037, 2004.

MacCarthy, P., The principles of humic substances, *Soil Sci.*, *166*, 738–751, 2001.

MacCarthy, P., C. E. Malcolm, and P. R. Bloom, An introduction to soil humic substances, in *Humic substances in Soil and Crop Sciences: Selected Readings*, edited by P. MacCarthy, C. E. Clapp, R. L. Malcolm, and P. R. Bloom, pp. 1–11, American Society of Agronomy, Soil Science Society of America, Madison, Wisconsin, 1990a.

MacCarthy, P., P. R. Bloom, C. E. Clapp, and R. L. Malcolm, Humic substances in soil and crop science: An overview, in *Humic substances in Soil and Crop Sciences: Selected Readings*, edited by P. MacCarthy, C. E. Clapp, R. L. Malcolm, and P. R. Bloom, pp. 261–271, American Society of Agronomy, Soil Science Society of America, Madison, Wisconsin, 1990b.

MacCarthy, P., R. L. Malcolm, C. E. Clapp, and P. R. Bloom, Spectroscopic methods (other than NMR) for determining functionality in humic substances, in *Humic Substances in Soil, Sediment and Water. Geochemistry, Isolation and Characteri-*

zation, edited by G. Aiken, D. McKnight, W. R., and P. MacCarthy, pp. 527–559, John Wiley, New York, 1985.

MacKenzie, K. J. D., R. H. Meinhold, I. W. M. Brown, and G. V. White, The formation of mullite from kaolinite under various reaction atmospheres, *J. Eur. Ceram. Soc.*, *16*, 115–119, 1996.

Magee, R. B., W. L. Lion, and T. A. Lemley, Transport of dissolved organic macromolecules and their effect on the transport of phenanthrene in porous media, *Environ. Sci. Technol.*, *25*, 323–331, 1991.

Mao, J., W. Hu, K. Schmidt-Rohr, G. Davies, E. A. Ghabbour, and B. Xing, Structure and elemental composition of humic acids: Comparison of solid-state ^{13}C NMR calculations and chemical analysis, in *Humic Substances Structure, Properties and Uses*, edited by G. Davies, and E. A. Ghabbour, pp. 79–90, The Royal Society of Chemistry, Cambridge, UK, 1998.

Marmur, A., Contact-angle hysteresis on heterogeneous smooth surfaces: theoretical comparison of the captive bubble and drop methods, *Colloids Surf. Physicochem. Eng. Aspects*, *136*, 209–215, 1998.

Márquez, G., M. J. P. Ribeiro, J. M. Ventura, and J. Labrincha, Removal of nickel from aqueous solutions by clay-based beds, *Ceram. Inter.*, *30*, 111–119, 1991.

McCarthy, J. F., Subsurface transport of dissolved humic substances and associated contaminants, in *Humic substances and Chemical Contaminats*, edited by C. E.

Clapp, M. H. B. Haynes, P. R. Senesi, and P. M. Jardine, pp. 429–448, Soil Science Society of America, Madison, Wisconsin, 2001.

Mekhamer, W. K., and F. F. Assaad, Thermodynamics of Sr-Mg vermiculite exchange and the effect of PVA on Mg release, *Thermochim. Acta*, *334*, 33–38, 1999.

Moen, D. E., and J. L. Richardson, Ultrasonic dispersion of soil aggregates stabilized by polyvinyl alcohol and T403-glyoxal polymers, *Soil Sci. Soc. Am. J.*, *48*, 628–631, 1984.

Murray, H. H., Traditional and new applications for kaolin, smectite, and palygorskite: A general overview, *Appl. Clay Sci.*, *17*, 207–221, 2000.

Nègre, M., P. Leone, C. Trichet, V. Boero, and M. Gennari, Characterization of model soil colloids by cryo-scanning electron microscopy, *Geoderma*, *121*, 1–16, 2004.

Nelson, S., J. Letey, W. Farmer, and M. Ben-Hur, Facilitated transport of napropamide by dissolved organic matter in sewage sludge-amended soil, *J. Environ. Qual.*, *27*, 1194–1200, 1998.

Nguyen, D. T., Determination of equilibrium surface energy of adsorbed polyvinyl alcohol layers in water at 25¸ *Colloids Surf. Physicochem. Eng. Aspects*, *116*, 145–160, 1996.

Oades, J. M., An introduction to organic matter in mineral soils, in *Humic substances in Soil and Crop Sciences: Selected Readings*, edited by J. B. Dixon, S. B. Weed,

and R. C. Dinauer, pp. 89–159, Soil Science Society of America, Madison, Wisconsin, 1989.

Saada, A., D. Breeze, C. Crouzet, S. Cornu, and P. Baranger, Adsorption of arsenic (V) on kaolinite and on kaolinitehumic acid complexes: Role of humic acid nitrogen groups, *Chemosphere*, *51*, 757–763, 2003.

Samoshina, Y., A. Diaz, Y. Becker, T. Nylander, and B. Lindman, Adsorption of cationic, anionic and hydrophobically modified polyacrylamides on silica surfaces, *Colloids Surf. Physicochem. Eng. Aspects*, *231*, 195–205, 2003.

Scheidegger, A., M. Borkovec, and H. Sticher, Coating of silica sand with goethite: Preparation and analytical identification, *Geoderma*, *14*, 777–793, 1993.

Schoen, R., J. Gaudet, and T. Bariac, Preferential flow and solute transport in a large lysimeter, controlled boundary conditions, *J. Hydrol. (Amsterdam)*, *215*, 70–81, 1999.

Schwertmann, U., and R. M. Cornell, *Iron Oxides in the Laboratory*, 2nd ed., Wiley-VCH, Weinheim, Germany, 2000.

Senesi, N., Nature of interaction between organic chemicals and dissolved humic substances and the influence of environmental factors, in *Organic Substances in Soil and Water. Natural Constituents and their Influences on Contaminant Behaviour*, edited by A. J. Beck, K. C. Jones, M. H. B. Hayes, and U. Mingelgrin, pp. 73–101, The Royal Society of Chemistry, Cambridge, UK, 1993.

Senesi, N., and E. Loffredo, Soil humic substances, in *Biopolymers*, edited by M. Hofrichter, and A. Steinbuchel, pp. 247–299, Wiley-Vch, Weinheim, Germany, 2001.

Shin, H., J. M. Monsallier, and G. R. Choppin, Spectroscopic and chemical characterizations of molecular size fractionated humic acid, *Talanta*, *50*, 641–647, 1999.

Shulten, H., A new approach to the structural analysis of humic substances in water and soils. Humic acids oligomers, in *Humic and Fulvic Acids: Isolation, Structure, and Environmental Role*, edited by J. Gaffney, N. Marley, and S. Clark, pp. 42–56, American Chemical Society, Washington, DC, 1996.

Simpson, A. J., R. E. Boersma, W. L. Kingery, R. P. Hicks, R. P. Hicks, and M. H. B. Haynes, Applications of NMR spectroscopy for studies of molecular compositions of humic substances, in *Organic Substances in Soil and Water. Natural Constituents and their Influences on Contaminant Behaviour*, edited by M. H. B. Hayes, and W. S. Wilson, pp. 46–62, The Royal Society of Chemistry, Cambridge, UK, 1997.

Sposito, G., *The Chemistry of Soils*, Oxford University Press, New York, 1989.

Sposito, G., On points of zero charge, *Environ. Sci. Technol.*, *32*, 2815–2819, 1998.

Spurlock, F. C., and J. W. Biggar, Effect of naturally-occurring soluble organic-matter on the adsorption and movement of simazine [2-chloro-4,6-bis(ethylamino)-s-triazine] in Hanford sandy loam, *Environ. Sci. Technol.*, *24*, 736–741, 1990.

Stahl, R. S., and B. R. James, Zinc sorption by iron-oxide-coated sand as a function of ph, *Soil Sci. Soc. Am. J.*, *55*, 1287–1290, 1991.

Steelink, C., What is humic acid? A perspective of the past forty years, in *Understanding Humic substances. Advances, Properties and Applications*, edited by E. A. Ghabbour, and G. Davies, pp. 1–8, The Royal Society of Chemistry, Cambridge, UK, 1999.

Stemme, S., and L. Ödberg, Layer thickness for high molecular weight cationic polyacrylamides adsorbed on a surface with a preadsorbed polydiallyldimethylammonium chloride, *Colloids Surf. Physicochem. Eng. Aspects*, *157*, 307–313, 1999.

Stemme, S., L. Ödberg, and M. Malmsten, Effect of colloidal silica and electrolyte on the structure of an adsorbed cationic polyelectrolyte layer, *Colloids Surf. Physicochem. Eng. Aspects*, *155*, 154–154, 1999.

Stevenson, F. J., *Humus Chemistry, Genesis, Composition, Reactions*, 2nd ed., John Wiley and Sons, New, York, USA, 1994.

Stott, D., and J. Martin, Synthesis and degradation of natural and synthetic humic material in soils, in *Humic Substances in Soil and Crop Sciences: Selected Readings*, edited by P. MacCarthy, C. E. Clapp, R. L. Malcolm, and P. R. Bloom, pp. 37–63, American Society of Agronomy, Soil Science Society of America, Madison, Wisconsin, 1990.

Stumm, W., *Chemistry of the Solid-Water Interface*, John Wiley & Sons, New York, 1992.

Swift, R., Macromolecular properties of humic substances: Fact, fiction, and opinion, *Soil Sci.*, *164*, 790–802, 1999.

Swift, R. S., Fractionation of soil humic substances, in *Humic Substances in Soil, Sediment and Water. Geochemistry, Isolation and Characterization*, edited by G. Aiken, D. McKnight, W. R., and P. MacCarthy, pp. 387–408, John Wiley, New York, 1985.

Swift, R. S., Organic matter characterization, in *Methods of Soil Analysis. Part 3: Chemical Methods*, edited by D. L. Sparks, pp. 1011–1069, Soil Science Society of America, Madison, USA, 1996.

Szabo, G., P. S. Lesley, and R. A. Bulman, Prediction of the adsorption coefficient (Koc) for soil by a chemically immobilized humic acid column using RP-HPLC, *Chemosphere*, *21*, 729–739, 1995.

Tadros, T. F., Adsorption of polyvinyl alcohol on silica at various pH values and its effect on the flocculation of the dispersion, *J. Colloid Interface Sci.*, *64*, 36–47, 1978.

Thang, N. M., H. Geckeis, J. I. Kim, and H. P. Beck, Application of the flow field flow fractionation (FFFF) to the characterization of aquatic humic colloids: evaluation

and optimization of the method, *Colloids Surf. Physicochem. Eng. Aspects*, *181*, 289–301, 2001.

Theng, B. K. G., *Formation and Properties of Clay-polymer Complexes*, Elsevier, Amsterdam, The Netherland, 1979.

Thomas, F., L. Michot, D. Vantelon, E. Montargès, B. Prélot, M. Cruchaudet, and J. Delon, Layer charge and electrophoretic mobility of smectites, *Colloids Surf. Physicochem. Eng. Aspects*, *159*, 351–358, 1999.

Thurman, E. A., and R. L. Malcolm, Preparative isolation of aquatic humic substances, *Environ. Sci. Technol.*, *15*, 463–466, 1981.

Tipping, E., *Cation Binding by Humic Substances*, Cambridge University Press, Cambridge, UK, 2002.

Toride, N., F. J. Leij, and M. T. van Genuchten, *The CXTFIT code for estimating transport parameters from laboratory or field experiments, Version 2.1*, Research Report 137, U.S. Salinity Laboratory, Riverside, CA, 1995.

Šimůnek, J., M. Šejna, and M. T. van Genuchten, *The HYDRUS-1D Software Package for Simulating the One-Dimensional Movement of Water, Heat and Multiple Solutes in Variably-Saturated Media*, U.S. Salinity Laboratory, Agricultural Research Service, U.S. Department of Agriculture, Riverside, CA, 1998.

Van de Weerd, H., W. H. Van Riemsdijk, and A. Leijnse, Modeling the dynamic adsorption desorption of a nom mixture: Effects of physical and chemical heterogeneity, *Environ. Sci. Technol.*, *33*, 1675–1681, 1999.

van Olphen, H., *An Introduction to Clay Colloid Chemistry*, 2nd ed., John Wiley, New York, 1977.

van Oss, C. J., *Interfacial Forces in Aqueous Media*, Dekker, New, York, USA, 1994.

von Wandruszka, R., The micellar model of humic acid: Evidence from pyrene fluorescence measurement, *Soil Sci.*, *163*, 921–930, 1998.

von Wandruszka, R., C. Ragle, and R. Engebretson, The role of selected cations in the formation of pseudomicelles in aqueous humic acid, *Talanta*, *44*, 805–809, 1997.

von Wandruszka, R., M. Schimpf, M. Hill, and R. Engebretson, Characterization of humic acid size fraction by SEC and MALS, *Org. Geochem.*, *30*, 229–235, 1999.

Vrancken, K. C., K. Possemiers, E. F. Van Der Voort, and E. F. Vansant, Surface modification of silica gels with aminoorganosilanes, *Colloids Surf. Physicochem. Eng. Aspects*, *98*, 235–241, 1995.

Wershaw, R., Application of Nuclear Magntic Resonance spectroscopy for determining functionality in humic substances, in *Humic Substances in Soil, Sediment and Water. Geochemistry, Isolation and Characterization*, edited by G. Aiken,

D. McKnight, W. R., and P. MacCarthy, pp. 561–582, John Wiley, New York, 1985.

Wershaw, R., *Membrane-Micelle Model for Humus in Soils and Sediments and its Relation to Humification*, vol. Water-supply paper 2410, US Geological Survey, USA, 1994.

Wershaw, R., and G. R. Aiken, Molecular size and weigh measurements of humic substances, in *Humic Substances in Soil, Sediment and Water. Geochemistry, Isolation and Characterization*, edited by G. Aiken, D. McKnight, W. R., and P. MacCarthy, pp. 561–582, John Wiley, New York, 1985.

Wershaw, R., and M. A. E. Mikita, *NMR of Humic Substances and Coal*, Lewis Publishers, Inc, Michigan, USA, 1987.

Wershaw, R. L., A new model for humic materials and their interactions with hydrophobic organic chemicals in soil-water or sediment-water systems, *J. Contam. Hydrol.*, *1*, 29–45, 1986.

Wershaw, R. L., Molecular aggregation of humic substances, *Soil Sci.*, *164*, 803–813, 1999.

Wershaw, R. L., and D. J. Pinckney, Chemical structure of humic acids – part 2. The molecular aggregation of some humic acids fractions in n,n-dimethylfolmamide, *J. Res. U.S. Geol. Surv.*, *5*, 571–577, 1977.

Wibulswas, R., Batch and fixed bed sorption of Methylene Blue on precursor and QACs modified montmorillonite, *Sep. Pur. Tech.*, *39*, 3–12, 2004.

Worrall, F., A. Parker, J. E. Rae, and A. C. Johnson, A study of suspended and colloidal matter in the leachate from lysimeters and its role in pesticide transport, *J. Environ. Qual.*, *28*, 595–604, 1999.

Wu, W., Baseline studies of the Clay Minerals Society source clays: Colloids and surface phenomena, *Clays Clay Miner.*, *49*, 446–452, 2001.

Xing, B., J. Mao, W. Hu, K. Schmidt-Rohr, G. Davies, and E. A. Ghabbour, Evaluation of different solid-state ^{13}C NMR techniques for characterizing humic acids, in *Understanding Humic Substances Advanced Methods, 'Properties and Applications*, edited by E. A. Ghabbour, and G. Davies, pp. 49–61, The Royal Society of Chemistry, Cambridge, UK, 1999.

Yang, Y., and L. K. Koopal, Immobilisation of humic acids and binding of nitrophenol to immobilised humics, *Colloids Surf. Physicochem. Eng. Aspects*, *151*, 201–212, 1999.